# SUPPLEMENTARY INFORMATION

# Interacting resonances and antiresonances in conjugated hydrocarbons: exceptional points and bound states in the continuum

N. M. Shubin[1], A. V. Emelianov[1,2], Yu. A. Uspenskii[1], and A. A. Gorbatsevich*[1]

[1]P.N. Lebedev Physical Institute of the Russian Academy of Sciences, 119991, Moscow, Russia.
[2]National Research University of Electronic Technology, 124498, Zelenograd, Moscow, Russia.

## Contents

**S1 Methods** **2**
S1.1 Details on analytical description . . . 2
S1.2 Details on numerical simulation . . . 3

**S2 Proportionate coupling** **3**

**S3 More illustrative examples within Hückel model** **3**
S3.1 Cyclobutadiene: destructive quantum interference and bound states in the continuum . . . 3
S3.2 Benzocyclobutadiene: coalescence of antiresonances . . . 5
S3.3 Cyclooctatetraene: bound states in the continuum . . . 6
S3.4 Anthracene: bound states in the continuum . . . 7
S3.5 Cyclobutadiene in para-configuration: bound state in the continuum by Friedrich-Wintgen mechanism 9

**S4 AR coalescence in cyclobutadiene with different side groups** **12**

**S5 Fitting DFTB simulations of CB by Hückel model** **12**

**S6 BIC in benzene with electrodes in para-configuration** **13**

**S7 Details on DFT simulations** **15**
S7.1 Pristine cyclobutadiene, $R = -0.29$ Å . . . 15
S7.2 Pristine cyclobutadiene, $R = 0.3$ Å . . . 17
S7.3 Cyclobutadiene with -$NH_2$ side groups, $R = -0.26$ Å . . . 19
S7.4 Cyclobutadiene with -$NH_2$ side groups, $R = 0.24$ Å . . . 21
S7.5 Pristine benzene in para-configuration . . . 23
S7.6 Benzene with -$NH_2$ side groups in para-configuration . . . 25

*gorbatsevichaa@lebedev.ru

# S1 Methods

## S1.1 Details on analytical description

Coherent current through the molecule and almost all transport properties are defined by its transmission coefficient $T(E)$, which can be calculated through the standard formula [S1]:

$$T\left(E\right)=4\,\mathrm{tr}\left[\hat{\Gamma}_r\hat{G}^r\left(E\right)\hat{\Gamma}_s\hat{G}^a\left(E\right)\right]. \tag{S1}$$

Here $\hat{G}^r(E)$ and $\hat{G}^a(E)=[\hat{G}^r(E)]^\dagger$ are, respectively, the retarded and the advanced Green's functions of the system. Matrices $\hat{\Gamma}_{s/r}$ define coherent coupling to the electrodes: $\hat{\Gamma}_{s/r}=\mathbf{u}_{s/r}\mathbf{u}_{s/r}^\dagger$ with

$$\mathbf{u}_s=\left(\gamma_1^s,\gamma_2^s,\ldots,\gamma_N^s\right)^\top,\quad \mathbf{u}_r=\left(\gamma_1^r,\gamma_2^r,\ldots,\gamma_N^r\right)^\top. \tag{S2}$$

In the stationary regime, the retarded Green's function can be calculated through the Feshbach's effective Hamiltonian $\hat{H}_{eff}$:

$$\hat{G}^r\left(E\right)=\left(\hat{I}E-\hat{H}_{eff}\right)^{-1}. \tag{S3}$$

In WBL the effective Hamiltonian is $\hat{H}_{eff}=\hat{H}_0-i\hat{\Gamma}_s-i\hat{\Gamma}_r$.

Our previous results [S2] showed that the transmission coefficient of any two-terminal quantum conductor could be rewritten in a more appropriate form for a resonance phenomena analysis:

$$T\left(E\right)=\frac{\left|P\left(E\right)\right|^2}{\left|P\left(E\right)\right|^2+\left|Q\left(E\right)\right|^2} \tag{S4}$$

with

$$P\left(E\right)=2\det\left(\hat{I}E-\hat{H}_0\right)\mathbf{u}_r^\dagger\left(\hat{I}E-\hat{H}_0\right)^{-1}\mathbf{u}_s, \tag{S5}$$

$$Q\left(E\right)=\det\left(\hat{I}E-\hat{H}_{aux}\right). \tag{S6}$$

Here $\hat{I}$ is the $N\times N$ identity matrix, and $\hat{H}_{aux}=\hat{H}_0+i\hat{\Gamma}_s-i\hat{\Gamma}_r$ is the auxiliary Hamiltonian of the system [S2].

Indeed, Eq. (S1) can be rewritten as

$$T(E)=4\left|\mathbf{u}_R^\dagger\left(E\hat{I}-\hat{H}_0+i\mathbf{u}_L\mathbf{u}_L^\dagger+i\mathbf{u}_R\mathbf{u}_R^\dagger\right)^{-1}\mathbf{u}_L\right|^2. \tag{S7}$$

Applying the Sherman-Morrison formula [S3] and the matrix determinant lemma [S4], one can simplify (S7) to

$$T=\frac{4\left|\det\left(E\hat{I}-\hat{H}_0\right)\right|^2\left|\mathbf{u}_R^\dagger\left(E\hat{I}-\hat{H}_0\right)^{-1}\mathbf{u}_L\right|^2}{\left|\det\left(E\hat{I}-\hat{H}_0+i\mathbf{u}_L\mathbf{u}_L^\dagger+i\mathbf{u}_R\mathbf{u}_R^\dagger\right)\right|^2}. \tag{S8}$$

Numerator of Eq. (S8) is nothing else than the $|P(E)|^2$ for $P(E)$ from Eq. (S5). Isolating the term $|P(E)|^2$ in the denominator of Eq. (S8) and applying the matrix determinant lemma once again one can figure out that

$$\left|\det\left(\omega\hat{I}-\hat{H}_{eff}\right)\right|^2=\left|\det\left(E\hat{I}-\hat{H}_0+i\mathbf{u}_L\mathbf{u}_L^\dagger+i\mathbf{u}_R\mathbf{u}_R^\dagger\right)\right|^2=|P(E)|^2+|Q(E)|^2, \tag{S9}$$

where $Q(E)$ is defined in Eq. (S6). Thus, one arrives to the transmission coefficient in the form (S4).

The proposed microscopic description of the interference phenomena in molecular conductors can be understood as a generalization of the source-sink potential (SSP) method [S5–S7], which refers the scattering problem in an open quantum system to an isolated system with additional complex potential describing incoming and outgoing currents.

### S1.2 Details on numerical simulation

DFTB+ package [S8] was used to calculate the optimal geometries, the density of states (DOS), and MOs. The SCC-DFTB method was utilized for calculations with Slater-Koster files auorg-1-1 [S9]. Geometry optimization was performed with $5 \times 10^{-3}$ Å/eV tolerance. Electron transmission was calculated using the non-equilibrium Green's function (NEGF) formalism. The contacts were treated within WBL approximation [S10].

To determine the optimized geometry, wavefunctions, and electron density more carefully, and to take into account the long-range electronic interaction, we performed DFT calculations using the Synopsys QuantumATK package version R-2020.09 [S11] at the PBE level of theory [S12, S13] with a linear combination of atomic orbitals (LCAO) and norm-conserving PseudoDojo pseudopotentials (High basis set) to expand the wave functions [S14]. Electron transport calculations were carried out via a combination of DFT and NEGF methods. The Monkhorst-Pack $k$-point grid of $3 \times 3 \times 401$ was used for the device transport calculations, whereas the electrode super-cell consisted of $3 \times 3 \times 2$ simple orthorhombic unit cells of Au fcc lattice in [111] direction. The energy grid cutoff was chosen to be 80 Hartree. The SCF convergence tolerance of $10^{-5}$ Hartree was used.

Molecular orbitals and geometries are plotted in VESTA program [S15] using 0.02 $(\text{e/Bohr})^{3/2}$ isovalue surface of charge density. The optimized geometries for DFT calculations are presented in Sec. S7.

## S2 Proportionate coupling

Consider a molecular conductor with proportionate coupling to the left and right leads: $\mathbf{u}_s = \lambda \mathbf{u}_r$ for some $\lambda \in \mathbb{C}$. In this case, it is appropriate to choose a basis, in which $\mathbf{u}_r$ becomes $\mathbf{u}_r = (\gamma, 0, ..., 0)^\top$. This can be done, for instance, by the Gram-Schmidt orthogonalization process. In this basis, from Eq. (S5), one can get:

$$P(E) = 2\lambda\gamma^2 \tilde{M}_{11}, \tag{S10}$$

where $\tilde{M}_{11}$ is the corresponding diagonal minor of the matrix $\hat{I}E - \hat{H}_0$ in the new basis.

Using the matrix determinant lemma [S4], one can simplify function $Q(E)$ from Eq. (S6) to:

$$Q(E) = \det\left[\hat{I}E - \hat{H}_0 + i\mathbf{u}_r\mathbf{u}_r^\dagger\left(1 - |\lambda|^2\right)\right] = \det\left(\hat{I}E - \hat{H}_0\right) + iP(E)\frac{1 - |\lambda|^2}{2}. \tag{S11}$$

Substituting Eqs. (S10-S11) into Eq. (S4), one can see that constructive quantum interference (resonances) take place at energies satisfying $\det(\hat{I}E - \hat{H}_0) = 0$, i.e. at MO energies of the molecule. However, resonant transmission is not perfect, in general, and its maximum value is $T_{max} = 4/[4 + (1 - |\lambda|^2)^2] \leq 1$.

In general, DQI is observed if $\tilde{M}_{11}$ turns to zero. In the case of point contacts, the new basis in which $\mathbf{u}_r$ takes the form $\mathbf{u}_r = (\gamma, 0, ..., 0)^\top$ is simply AO basis. Thus, in this case, conditions for DQI $\tilde{M}_{11} = 0$ is satisfied at the energies of the reduced molecule as proposed in the main text.

## S3 More illustrative examples within Hückel model

### S3.1 Cyclobutadiene: destructive quantum interference and bound states in the continuum

Isolated molecule of CB is a diradical and has two degenerate NBOs (in a perfectly square geometry). Thus, it can be used to illustrate the possibility for BIC formation from one of the NBOs. Consider a CB molecule side-coupled to a linear chain (Fig. S1a). This structure corresponds to the general case shown in Fig. 2 of the main text with

$$\hat{H}_0 = \begin{pmatrix} \varepsilon_0 & -\tau & 0 & -\tau_0 & -\tau_1 \\ -\tau & \varepsilon_0 & -\tau_0 & 0 & 0 \\ 0 & -\tau_0 & \varepsilon_0 & -\tau & 0 \\ -\tau_0 & 0 & -\tau & \varepsilon_0 & 0 \\ -\tau_1 & 0 & 0 & 0 & \varepsilon_0 \end{pmatrix} \tag{S12}$$

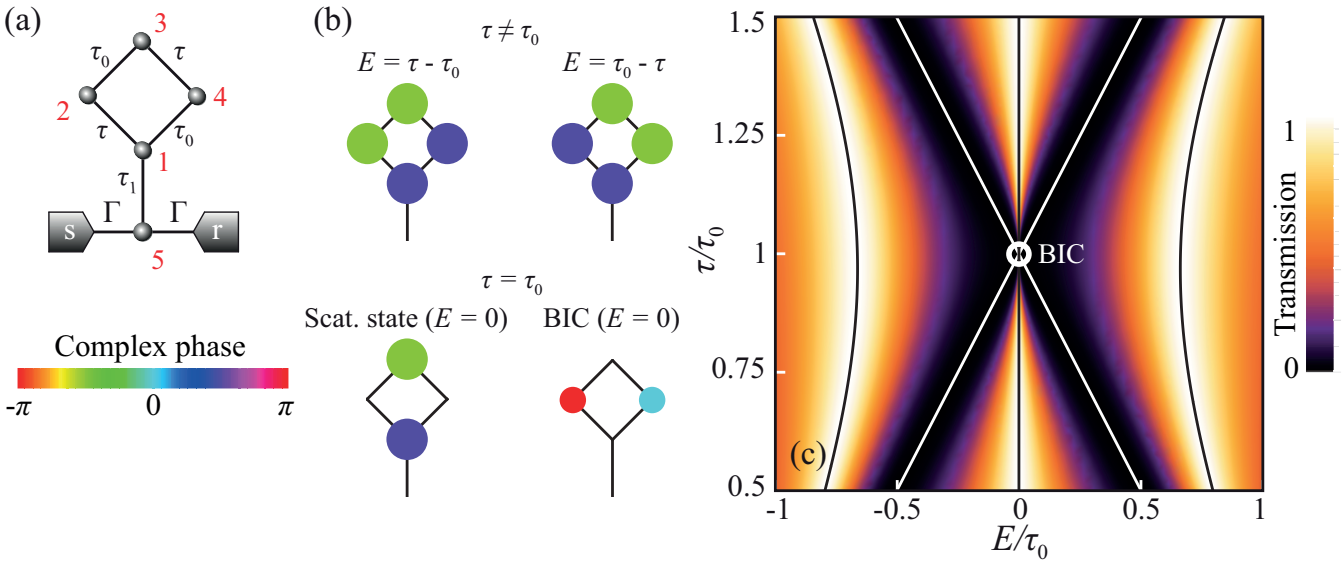


Figure S1: (a) Carbon skeleton of CB side-coupled to a linear chain as a graph for Hückel model. (b) Transformation of the scattering state wavefunction in CB molecule with BIC formation. The absolute value of the site amplitude corresponds to the radius of the circle and complex phase – to its color. (c) Density plot of the transmission coefficient evolution with varying $\tau/\tau_0$ ratio for $\Gamma = 0.3\tau_0$. Black lines indicate perfect resonances, white lines show the position of zero ARs. BIC formation takes place, where these lines intersect (shown by a white open circle).

in AO basis and $\hat{H}_0' = \hat{H}_0^{CB}$, where $\hat{H}_0^{CB}$ is the Hamiltonian of CB molecule:

$$\hat{H}_0' = \hat{H}_0^{CB} = \begin{pmatrix} \varepsilon_0 & -\tau & 0 & -\tau_0 \\ -\tau & \varepsilon_0 & -\tau_0 & 0 \\ 0 & -\tau_0 & \varepsilon_0 & -\tau \\ -\tau_0 & 0 & -\tau & \varepsilon_0 \end{pmatrix} \tag{S13}$$

Couplings to electrodes are equal: $\mathbf{u}_{s,r} = (0,0,0,0,\sqrt{\Gamma})^\top$. We again set $\varepsilon_0$ as energy origin. In agreement with the Coulson-Rushbrooke theorem, Hamiltonian (S12) has an eigenvalue $E = \varepsilon_0 = 0$ regardless the value of hoppings $\tau$, $\tau_0$, and $\tau_1$ because it corresponds to an alternant hydrocarbon with odd number of carbon atoms. Hamiltonian $\hat{H}_0' = \hat{H}_0^{CB}$, have eigenvalues at $E_{DQI} = \pm(\tau_0 - \tau)$, which become degenerate at $E = 0$ for $\tau = \tau_0$. Thus, according to Eqs. (20) of the main text a BIC formation at $E = 0$ and for $\tau = \tau_0$ is expected because functions $P(E)$ and $Q(E)$ will have a common root in this case. Indeed, using Eqs. (20) of the main text, one can calculate the transmission coefficient of this system (see Fig. S1c) and admit the collapse of resonance and antiresonance at $E = 0$ and $\tau = \tau_0$, which indicates the BIC.

In the energy-parameters space, formation of a BIC corresponds to a discontinuity point of the transmission coefficient and wavefunctions [S2, S16]. Let us solve the scattering problem for the system under consideration and derive the wavefunction of the scattering state (state with scattering boundary conditions) with a particular energy. To do so, we will use the formalism of Ref. [S17] and find the scattering state wavefunction $\mathbf{a} \in \mathbb{C}^5$ as

$$\mathbf{a} = \left(\hat{I}E - \hat{H}_0 + i\mathbf{u}_s\mathbf{u}_s^\dagger + i\mathbf{u}_r\mathbf{u}_r^\dagger\right)^{-1}\mathbf{s}, \tag{S14}$$

where $\mathbf{s} = (0,0,0,0,2i\sqrt{\Gamma})^\top$ is the "source vector" in AO basis, which is due to the incident electron boundary conditions. For $\tau \neq \tau_0$ at energies of ARs $E_{DQI} = \pm(\tau - \tau_0)$ we have $\mathbf{a} = 2i\sqrt{\Gamma}/\tau_1(1, \mp 1, -1, \pm 1, 0)^\top$ (see the first row in Fig. S1b). These scattering states continue to exist even if the difference $|\tau - \tau_0|$ is infinitesimal. Exactly at $\tau = \tau_0$ the scattering state changes abruptly to $\mathbf{a} = 2i\sqrt{\Gamma}/\tau_1(1,0,-1,0,0)^\top$ and the BIC wavefunction forms orthogonal to the scattering state $\mathbf{a}_{BIC} = 1/\sqrt{2}(0,-1,0,1,0)^\top$ (see the second row in Fig. S1b). Such an abrupt change is a manifestation of BIC as a discontinuity point [S2].

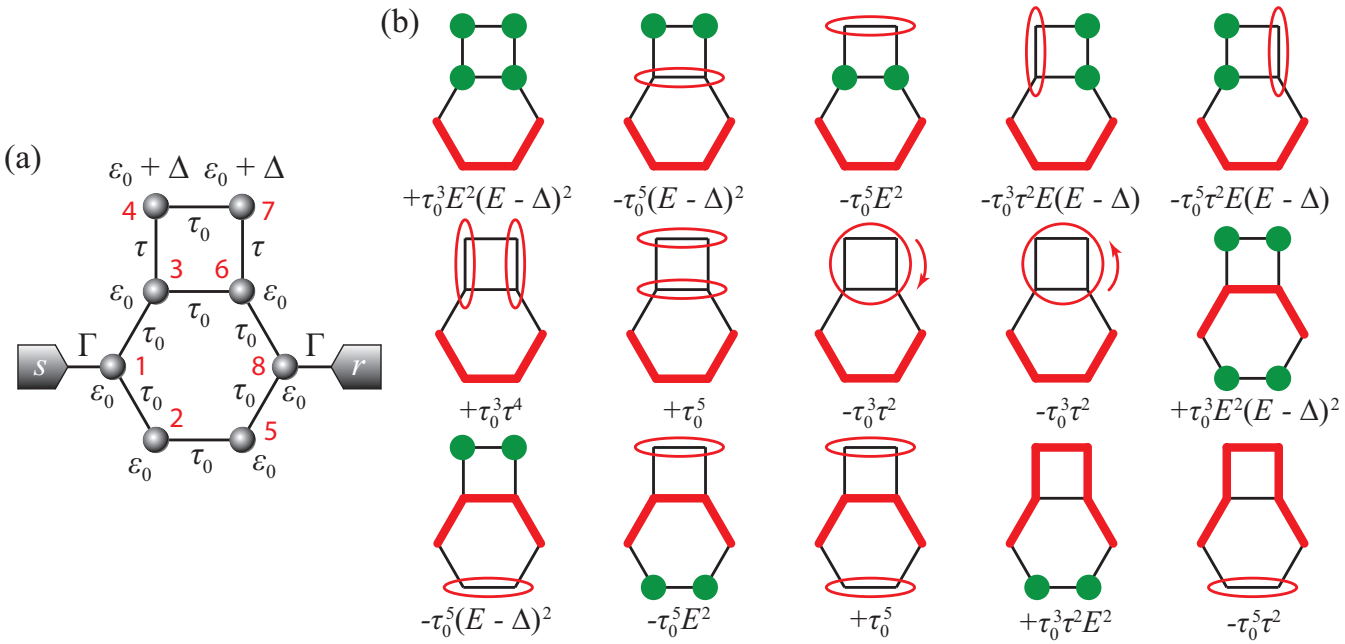


Figure S2: (a) Schematic view of the BCB molecule connected to two leads. (b) AO diagrams for calculating the numerator of the transmission coefficient [S18]

## S3.2 Benzocyclobutadiene: coalescence of antiresonances

Consider the molecule of benzocyclobutadiene (BCB) connected to two identical leads. Suppose also that two carbon atoms are affected by the gate and have $2p_z$-orbital energies shifted by $\Delta$ as shown in Fig. S2a. The bare Hamiltonian of the molecule in the atomic orbital (AO) basis (as numbered in Fig. S2a) is the following:

$$\hat{H}_0 = \begin{pmatrix} \varepsilon_0 & -\tau_0 & -\tau_0 & 0 & 0 & 0 & 0 & 0 \\ -\tau_0 & \varepsilon_0 & 0 & 0 & -\tau_0 & 0 & 0 & 0 \\ -\tau_0 & 0 & \varepsilon_0 & -\tau & 0 & -\tau_0 & 0 & 0 \\ 0 & 0 & -\tau & \varepsilon_0+\Delta & 0 & 0 & -\tau_0 & 0 \\ 0 & -\tau_0 & 0 & 0 & \varepsilon_0 & 0 & 0 & -\tau_0 \\ 0 & 0 & -\tau_0 & 0 & 0 & \varepsilon_0 & -\tau & -\tau_0 \\ 0 & 0 & 0 & -\tau_0 & 0 & -\tau & \varepsilon_0+\Delta & 0 \\ 0 & 0 & 0 & 0 & -\tau_0 & -\tau_0 & 0 & \varepsilon_0 \end{pmatrix}. \tag{S15}$$

On-site energy $\varepsilon_0$ we set as energy origin. Coupling to the leads are described by the following vectors in AO basis within the WBL approximation:

$$\mathbf{u}_s = \begin{pmatrix} \sqrt{\Gamma} & 0 & 0 & 0 & 0 & 0 & 0 & 0 \end{pmatrix}^\top, \quad \mathbf{u}_r = \begin{pmatrix} 0 & 0 & 0 & 0 & 0 & 0 & 0 & \sqrt{\Gamma} \end{pmatrix}^\top. \tag{S16}$$

Here $\Gamma$ defines the coupling strength with the left/right lead.

Using general formalism [S2] for description of coherent transport through quantum conductors, one can calculate the transmission coefficient of BCB in the following form [see Eq. (S4)]:

$$T_{BCB}(E) = \frac{|P_{BCB}(E)|^2}{|P_{BCB}(E)|^2 + |Q_{BCB}(E)|^2}. \tag{S17}$$

Here $P_{BCB}(E)$ and $Q_{BCB}(E)$ we calculate using Eqs. (S5-S6):

$$\begin{aligned}
P_{BCB}(E) &= 2\Gamma\tau_0^3\left[2E^2(E-\Delta)^2 - E^2\left(\tau^2+4\tau_0^2\right) + 2\Delta E\left(\tau^2+2\tau_0^2\right) + \left(\tau^2-\tau_0^2\right)^2 + \tau_0^2\left(\tau_0^2-\tau^2-2\Delta^2\right)\right],\\
Q_{BCB}(E) &= E^6(E-\Delta)^2 - E^6\left(2\tau^2+7\tau_0^2-\Gamma^2\right) + 2\Delta E^5\left(\tau^2+6\tau_0^2-\Gamma^2\right)\\
&+ E^4\left[\left(\tau^2+3\tau_0^2\right)^2 + 3\tau_0^2\left(\tau_0^2-2\Delta^2-\Gamma^2\right) - 2\Gamma^2\tau^2\right] - 2\Delta E^3\left[\tau_0^2\left(4\tau^2+9\tau_0^2\right) - \Gamma^2\left(\tau^2+2\tau_0^2\right)\right]\\
&- E^2\left[\tau^4\left(3\tau_0^2-\Gamma^2\right) + \tau_0^2\left(13\tau_0^4 - 9\Delta^2\tau_0^2 - 3\Gamma^2\tau_0^2 + 2\Delta^2\Gamma^2\right)\right] + 2\Delta\tau_0^2E\left[\tau_0^2\left(3\tau^2+4\tau_0^2-\Gamma^2\right) - \Gamma^2\tau^2\right]\\
&+ \tau^4\tau_0^4 - 4\left(\Delta^2+\tau^2\right)\tau_0^6 + 4\tau_0^8 - \Gamma^2\tau_0^2\left[\tau^4 - \left(\Delta^2+2\tau^2\right)\tau_0^2 + \tau_0^4\right].
\end{aligned} \tag{S18}$$

One can also derive numerator of the transmission coefficient, i.e., function $P_{BCB}$ (except for $2\Gamma$ prefactor) following the graphical rules from Ref. [S18] (see Figure S2b). Such graphical rules are illustrative and do shed light on the physical mechanisms only in the case of single ARs [S19]. On the other hand, one have to sum almost up all these diagrams to be able to describe AR coalescence phenomenon. For example, summation of 14 diagrams (out of 15) is required for BCB. Hence, in this case AO diagrams cannot provide any illustrative and easy-to-understand description of this phenomenon. Moreover, one should be aware that diagrammatic methods proposed in Refs. [S18, S20] are valid only in the case of point contacts, i.e., for electrodes, which interact with the molecule through only one atom each. In general, numerator of the transmission coefficient does not have the form of a minor of some characteristic determinant in AO basis [S2], which was assumed for derivation of these graphical rules.

Consider now the evolution of the transmission spectra with varying $\tau/\tau_0$ ratio for $\Delta = 0$. In this case function $P_{BCB}(E)$ from Eq. (S18) simplifies to

$$P_{BCB}(E) = 2\Gamma\tau_0^3\left[2E^4 - E^2\left(\tau^2+4\tau_0^2\right) + \left(\tau^2-\tau_0^2\right)\left(\tau^2-2\tau_0^2\right)\right]. \tag{S19}$$

From this equation one can see that in the vicinity of Fermi energy (which is typically assumed to be close to $\varepsilon_0$, i.e., zero in our notation), there are two zeroes of $P_{BCB}(E)$, and hence two ARs in the transmission for $\tau/\tau_0 \in (0,1)\cup(\sqrt{2},+\infty)$. If $\tau/\tau_0 \in (1,\sqrt{2})$, then there is no real roots of $P_{BCB}$ near $E=0$ and hence no zero-valued transmission dips are observed. Such change of behavior takes place due to AR coalescence at $\tau = \tau_0$ and $\tau = \sqrt{2}\tau_0$.

Figure S3a depicts the evolution of the BCB transmission coefficient with varying $\tau/\tau_0$ ratio for $\Delta = 0$ and $\Gamma = 0.3\tau_0$. Solid white lines correspond to the exact positions of zero-valued ARs, which coalesce at $\tau = \tau_0$ and $\tau = \sqrt{2}\tau_0$. Dashed white lines show approximate AR positions from Eq. (9) of the main text. This approximation corresponds to eigenvalues of $\hat{H}_{\mathcal{PT}}$ from Eq. (14) of the main text. Thus, $\mathcal{PT}$-symmetry breaking of $\hat{H}_{\mathcal{PT}}$ at its EPs qualitatively describes AR coalescence at $\tau = \tau_0$ and $\tau = \sqrt{2}\tau_0$.

BCB also possesses AR coalescence for energy shift of two carbon atoms $2p_z$-orbitals (by gating). This effect takes place for $\tau < \tau_0$ (or, equivalently, for $\tau > \sqrt{2}\tau_0$) and $\Delta \neq 0$. For certainty, we focus on the case $\tau < \tau_0$. Fig. S3b shows the evolution of the BCB transmission coefficient spectrum with varying $\Delta$ for $\tau = 0.95\tau_0$ and $\Gamma = 0.3\tau_0$. Solid white lines correspond to the exact positions of zero-valued ARs, which coalesce at $\Delta \approx 0.68807\tau_0$. Dashed white lines show approximate AR positions from Eq. (9) of the main text.

### S3.3 Cyclooctatetraene: bound states in the continuum

Consider the molecule of cyclooctatetraene (COT) connected to two identical electrodes (Fig. S4a) via equal couplings $\Gamma$. The Hamiltonian of the isolated COT molecule is the following

$$\hat{H}_0 = \begin{pmatrix}
\varepsilon_0 & -\tau & 0 & 0 & 0 & 0 & 0 & -\tau\\
-\tau & \varepsilon_0 & -\tau & 0 & 0 & 0 & 0 & 0\\
0 & -\tau & \varepsilon_0 & -\tau & 0 & 0 & 0 & 0\\
0 & 0 & -\tau & \varepsilon_0 & -\tau & 0 & 0 & 0\\
0 & 0 & 0 & -\tau & \varepsilon_0 & -\tau & 0 & 0\\
0 & 0 & 0 & 0 & -\tau & \varepsilon_0 & -\tau & 0\\
0 & 0 & 0 & 0 & 0 & -\tau & \varepsilon_0 & -\tau\\
-\tau & 0 & 0 & 0 & 0 & 0 & -\tau & \varepsilon_0
\end{pmatrix}. \tag{S20}$$

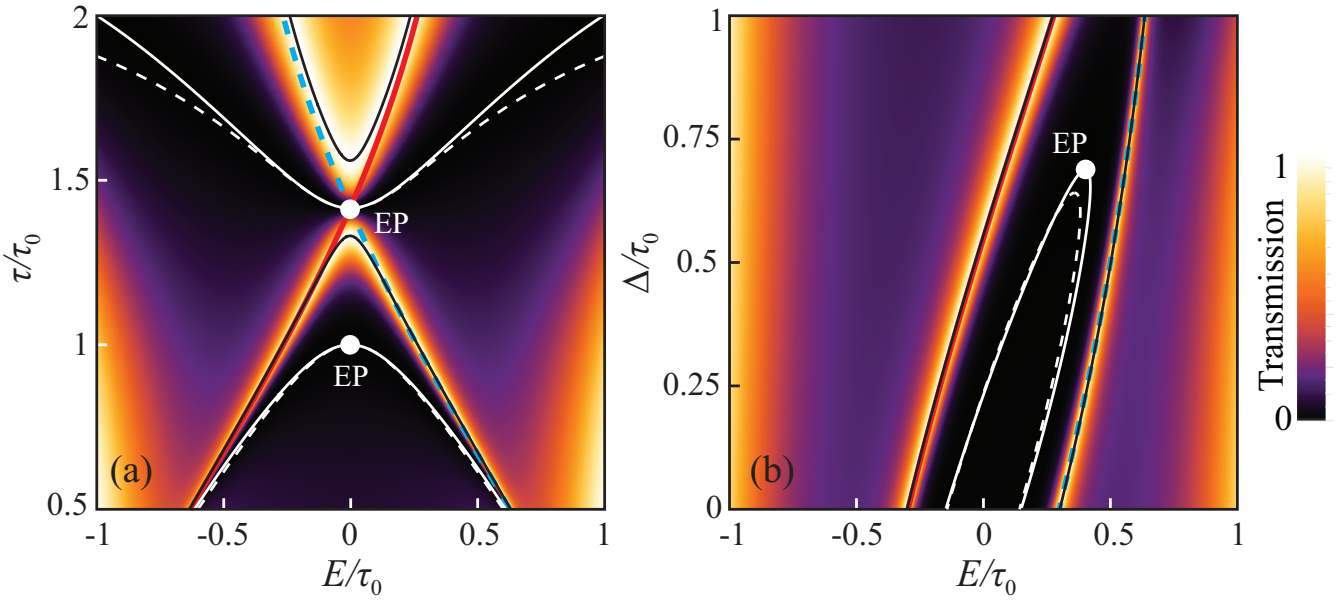


Figure S3: Evolution of the transmission coefficient spectrum with (a) varying $\tau/\tau_0$ ratio for $\Delta = 0$ and $\Gamma = 0.3\tau_0$ and (b) varying $\Delta$ for $\tau = 0.95\tau_0$ and $\Gamma = 0.3\tau_0$. Black lines correspond to the positions of perfect transmission resonances, solid white lines – positions of zero-valued antiresonances, and dashed white line show approximate AR positions from Eq. (9) of the main text. Solid red and dashed blue lines indicate energy levels of symmetric/antisymmetric MOs correspondingly.

According to graphical rules [S18] or using Eq. (S5), one can conclude that the numerator of the transmission coefficient $P(E)$ turns to zero at $E = \varepsilon_0 = 0$ for any configuration of the electrodes attachment (Fig. S4a). Thus, one may conclude that DQI can be observed at this energy regardless the configuration. However, this is not true.

Within the nearest-neighbor approximation and taking all tunneling matrix elements in the cycle to be the same (we label it as $\tau$) one can calculate functions $P(E)$ and $Q(E)$ from Eqs. (S5-S6) for any configuration of the leads. In the 1-2 and 1-4 configurations functions $P_{12}(E)$ and $P_{14}(E)$ turn to zero at $E = 0$, whereas $Q_{12}(E = 0)$ and $Q_{14}(E = 0)$ remain finite. Therefore, there is DQI (hard zero) at $E = 0$ in 1-2 and 1-4 configurations, as was predicted by graphical rules. In 1-3 and 1-5 configurations we have:

$$\begin{aligned} P_{13}(E) &= 2\tilde{E}\tilde{\Gamma}\left(\tilde{E}^2 - 2\right)^2, \quad Q_{13}(E) = \tilde{E}^2\left[\tilde{E}^6 - \tilde{E}^4\left(8 - \tilde{\Gamma}^2\right) + 4\tilde{E}^2\left(5 - \tilde{\Gamma}^2\right) - 16 + 3\tilde{\Gamma}^2\right], \\ P_{15}(E) &= 2\tilde{E}\tilde{\Gamma}\left(\tilde{E}^2 - 2\right), \quad Q_{15}(E) = \tilde{E}^2\left[\tilde{E}^6 - \tilde{E}^4\left(8 - \tilde{\Gamma}^2\right) + 4\tilde{E}^2\left(5 - \tilde{\Gamma}^2\right) - 4\left(4 - \tilde{\Gamma}^2\right)\right], \end{aligned} \tag{S21}$$

where we use $\tilde{E} = E/\tau$ and $\tilde{\Gamma} = \Gamma/\tau$ for short. $P_{13}(E)$ and $P_{15}(E)$ also turn to zero at $E = 0$. However, $E = 0$ is the second order root of $Q_{13}(E)$ and $Q_{15}(E)$, which implies that there is a BIC at $E = 0$ and the transmission coefficient at this energy is perfect (equal to unity) in the 1-3 and 1-5 configurations. This fact is non-trivial because in 1-3 and 1-5 configurations the leads are attached to atoms of the same subset (both starred or unstarred), and hence the formation of an easy zero is highly expected [S21].

Thus, we show that analysis of only the numerator of the transmission coefficient can result in spurious ARs, which do not exist in fact because of BIC formation. Figures S4b,c depict BIC and scattering wavefunctions for 1-3 and 1-5 configurations. BIC and scattering wavefunctions are orthogonal as expected and the last possess symmetric electron density distribution, which indicates perfect transmission.

### S3.4 Anthracene: bound states in the continuum

Consider the anthracene molecule coupled to two identical electrodes via equal couplings $\Gamma$ as in Fig. S5a. The bare Hückel Hamiltonian of the isolated molecule can be easily written from this schematic graph. Suppose that two carbon atoms are affected by gating, which introduces the on-site energy shift $\Delta$ (Fig. S5a). Without perturbation

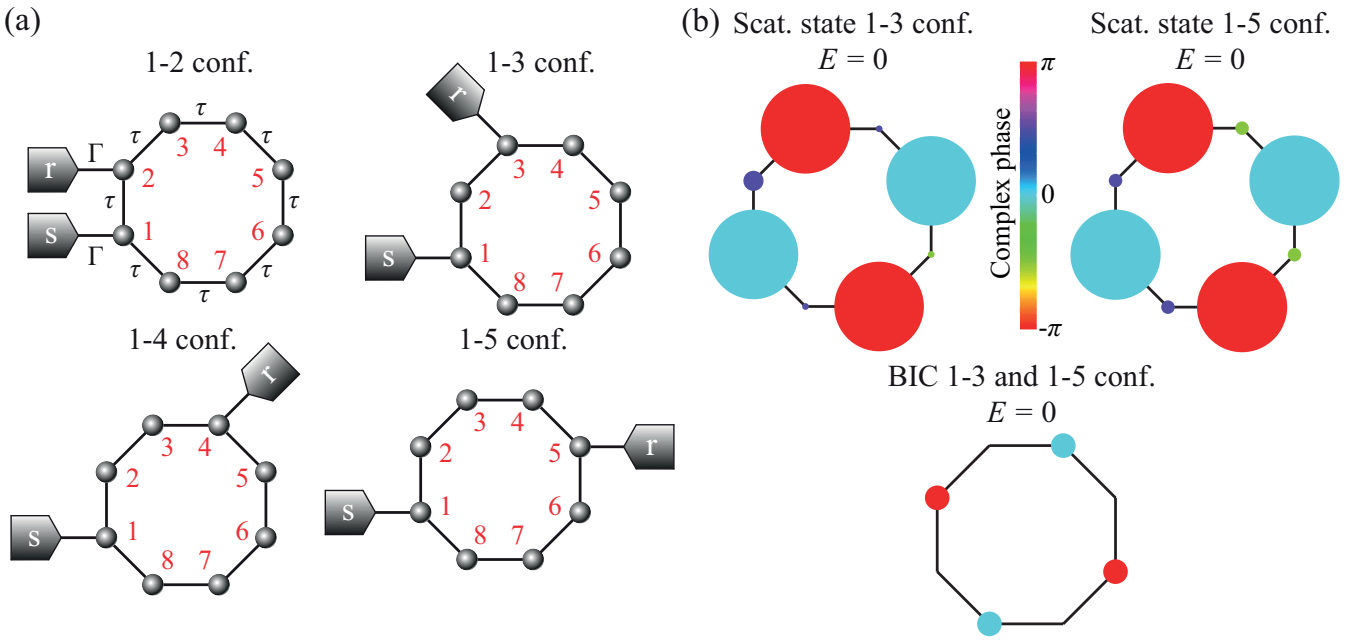


Figure S4: (a) Carbon skeleton of COT as a graph for Hückel model. (b) BIC and (c) scattering state wavefunctions in COT molecule for 1-3 and 1-5 electrodes configuration. Absolute value of the site amplitude corresponds to the radius of the circle and complex phase – to its color. We set $\Gamma = 0.3\tau$.

($\Delta = 0$) there are four pairs of degenerate MOs at energies $E = \varepsilon_0 \pm \tau$ and $E = \varepsilon_0 \pm \sqrt{2}\tau$. We focus on the pair at energy $E = \varepsilon_0 - \tau$ (similar conclusions can be made for the pair at energy $E = \varepsilon_0 + \tau$). One of the orbitals in this pair vanishes at the 3rd and the 4th carbon atoms and hence has zero couplings with electrodes, which means that it is a BIC (Fig. S5b). Non-zero gating lifts the degeneracy. One can calculate that for $\Delta \neq 0$ MOs have non-vanishing amplitudes on sites 3 and 4 (Fig. S5b). Thus, BIC is formed in the degenerate case by the Friedrich-Wintgen mechanism [S22].

Without perturbation functions $P(E)$ and $Q(E)$ can be calculated as follows:

$$\begin{aligned} P(E) =& 4\Gamma\tau^3\left(E^{10} - 10E^8\tau^2 + 34E^6\tau^4 - 50E^4\tau^6 + 31E^2\tau^8 - 6\tau^{10}\right), \\ Q(E) =& \left(E^2-\tau^2\right)^2\left[E^{10} + E^8\left(\Gamma^2 - 14\tau^2\right) + E^6\left(69\tau^4 - 10\Gamma^2\tau^2\right) + E^4\left(31\Gamma^2\tau^4 - 144\tau^6\right) + E^2\left(116\tau^8 - 34\Gamma^2\tau^6\right)\right. \\ & \left. + \tau^8\left(9\Gamma^2 - 16\tau^2\right)\right]. \end{aligned} \tag{S22}$$

Here we again set $\varepsilon_0$ as energy origin. These $P(E)$ and $Q(E)$ functions has a common root at $E = -\tau$ as it should be in the case of BIC. Moreover, one can see that $E = -\tau$ is a simple root of $P(E)$ and a second-order root of $Q(E)$. Hence, the transmission coefficient is equal unity at this energy. In the presence of non-zero perturbation expressions for $P(E)$ and $Q(E)$ functions become cumbersome. However, it is illustrative to study their properties in the vicinity of $E = -\tau$ and $\Delta = 0$. Thus, one can study the behavior of their roots with increasing $\Delta$. Function $P(E)$ turns to zero at a real energy, which approximately is $E_P \approx -\tau + \Delta/8$. On the other hand, roots of function $Q(E)$ become complex for $\Delta \neq 0$: $E_Q^{1,2} \approx -\tau + C_{1,2}\Delta$, where $C_{1,2} \in \mathbb{C}$. Thus, there are no perfect transmission resonances in the perturbed system, because perturbation makes the system non-symmetric with respect to the mirror reflection mapping electrodes into each other. In Fig. S5c, there is a density plot of the transmission coefficient spectrum evolution with varying $\Delta$. It should also be noted that there is no BIC at $E = -\sqrt{2}\tau$ for $\Delta = 0$ because conditions for the Friedrich-Wintgen mechanism are not fulfilled. However, function $P(E)$ turns to zero at this point in full agreement with the general formula (5) in the main text, and hence there is an AR (see Fig. S5c).

It is important to note that taking the next-nearest neighbors into account prevents BIC formation. In this case, any MO will have non-zero amplitude on the 3rd and the 4th atoms, which prevents it from turning into BIC.

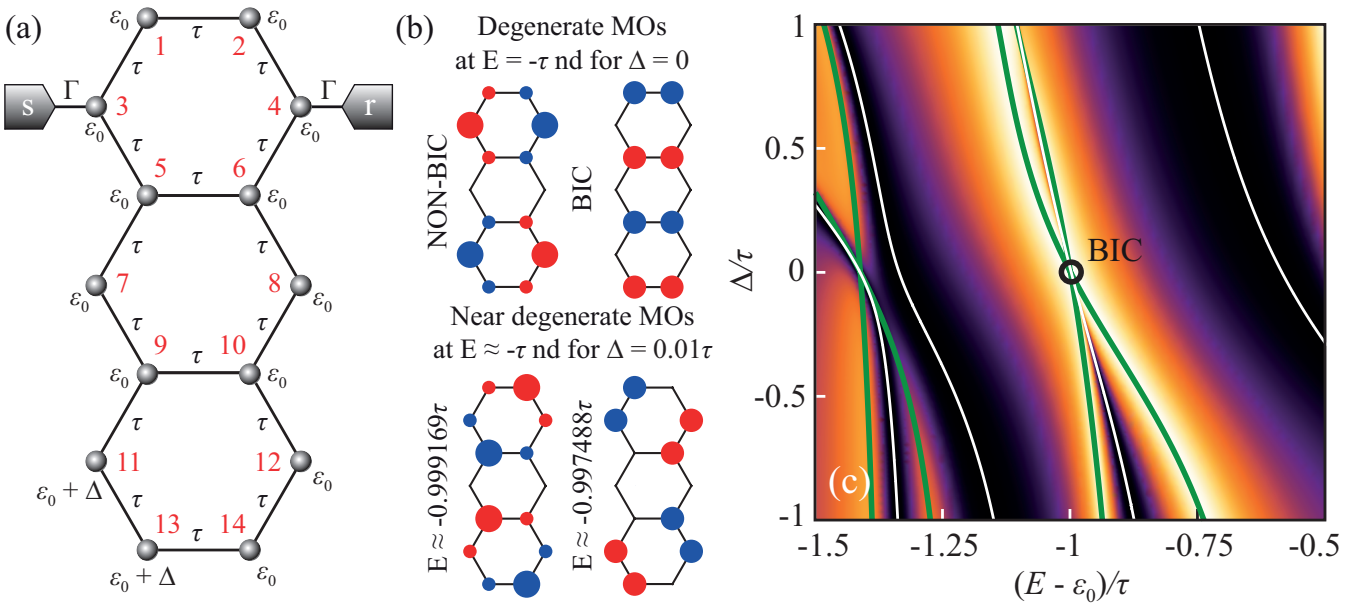


Figure S5: (a) Carbon skeleton of anthracene as a graph for Hückel model. (b) Degenerate MOs one of which is BIC at $E = -\tau$ without perturbation and MOs with non-vanishing coupling to electrodes in slightly perturbed system ($\Delta = 0.01\tau$). (c) Evolution of the transmission coefficient spectrum with varying $\Delta/\tau$ ratio for $\Gamma = 0.3\tau$. White lines correspond to positions of zero-valued antiresonances and thick green lines show MOs energies.

### S3.5 Cyclobutadiene in para-configuration: bound state in the continuum by Friedrich-Wintgen mechanism

Consider the CB molecule coupled to two electrodes in a para-configuration (Fig. S6a). The bare Hückel Hamiltonian of the considered molecule is

$$\hat{H}_0 = \begin{pmatrix} \varepsilon_0 & -\tau & -\tau_1 & -\tau \\ -\tau & \varepsilon_0 + \Delta & -\tau & -\tau_2 \\ -\tau_1 & -\tau & \varepsilon_0 & -\tau \\ -\tau & -\tau_2 & -\tau & \varepsilon_0 - \Delta \end{pmatrix}. \tag{S23}$$

Here we take into account the next-nearest-neighbors hoppings $\tau_{1,2}$ and suppose an external gating energy shift $\Delta$. Form Eq. (S23), one can see that without external gating ($\Delta = 0$) there is no degenerate MOs for $\tau_1 \neq \tau_2$, $\tau_1 \neq 2\tau^2/\tau_2 - \tau_2$ and $\tau_2 \neq 2\tau^2/\tau_1 - \tau_1$.

Coupling to electrodes in para-configuration through matrix elements $\Gamma$ implies the following expressions for functions $P(E)$ and $Q(E)$:

$$\begin{aligned} P(E) =& 2\Gamma\left\{\Delta^2\tau_1 - (E-\tau_2)\left[\tau_1(E+\tau_2) - 2\tau^2\right]\right\}, \\ Q(E) =& (E-\tau_2)\left[E^3 + E\Gamma^2 - 4E\tau^2 + 4\tau^2\tau_1 - E\tau_1^2 + \left(E^2 + \Gamma^2 - \tau_1^2\right)\tau_2\right] - \Delta^2\left(E^2 + \Gamma^2 - \tau_1^2\right). \end{aligned} \tag{S24}$$

Analyzing Eqs. (S24), one can conclude that $P(E)$ and $Q(E)$ have a common root $E = \tau_2$ for $\Delta = 0$. Thus, there is a BIC for $\Delta = 0$ at energy $E = \tau_2$, whereas no degeneracy takes place. The wavefunction of BIC is shown in Fig. S6b. This is a generalized Friedrich-Wintgen mechanism [S22] for interacting localized states. The realization of such a BIC formation mechanism in the cyclobutadiene molecule in para-configuration can be regarded as a generalization of a simple two-site model studied in Ref. [S23].

Figure S6c depicts an example of the transmission spectrum evolution with varying $\Delta$ for the system with $\tau_1 = 0.1\tau$, $\tau_2 = 0.2\tau$, and $\Gamma = 0.3\tau$. One can see that no degeneracy takes place, but nevertheless BIC is formed.

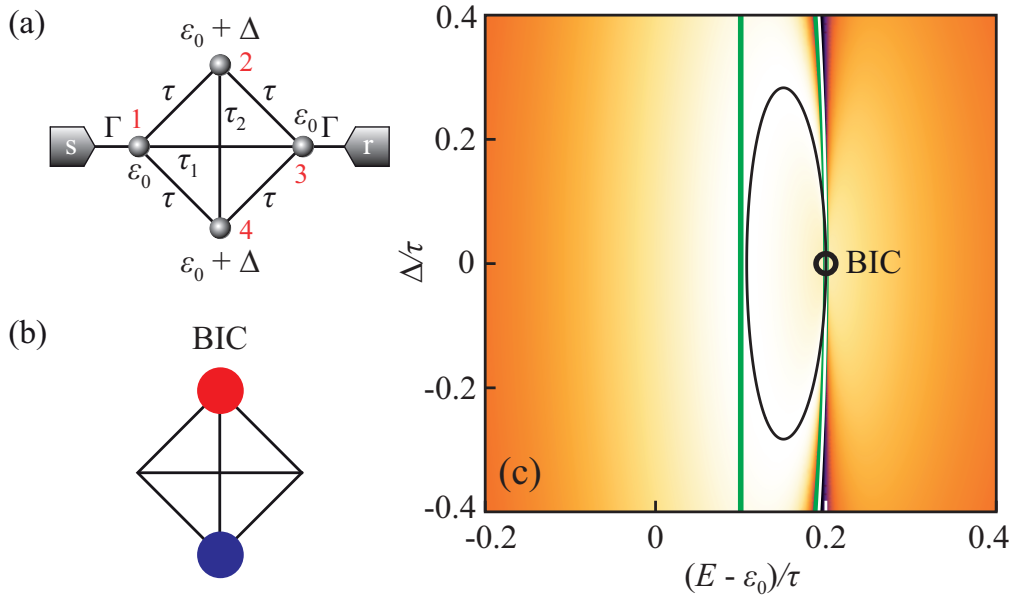


Figure S6: (a) Carbon skeleton of CB in para-configuration as a graph for Hückel model beyond the nearest-neighbor appeoximation. (b) BIC wavefunction in CB molecule in para-configuration. (c) Evolution of the transmission coefficient spectrum with varying $\Delta/\tau$ ratio. White lines correspond to positions of zero-valued antiresonances, black lines – unity-valued resonances, and thick green lines show MOs energies.

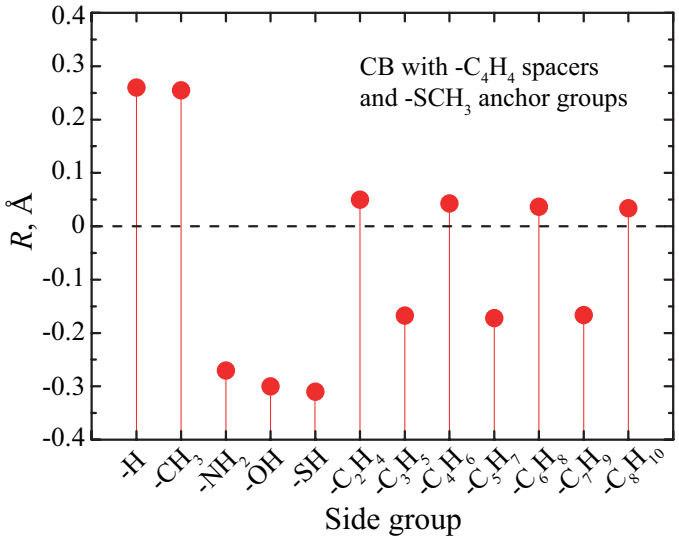


Figure S7: $R$ parameter of the optimal geometry (corresponding to the global minimum of the total energy) as a function of side group in the CB molecule.

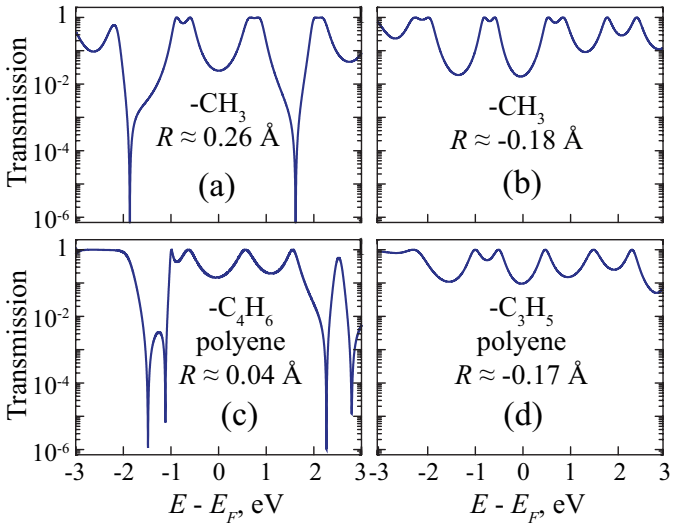


Figure S8: (a, b) Transmittance of CB with -$CH_3$ side groups at two local minimums of the total energy. Global minimum corresponds to the case (a) with $R \approx 0.26$ Å. Transmission of CB with -$C_4H_6$ (a) and -$C_3H_5$ polyene side groups at corresponding global minimums of the total energy.

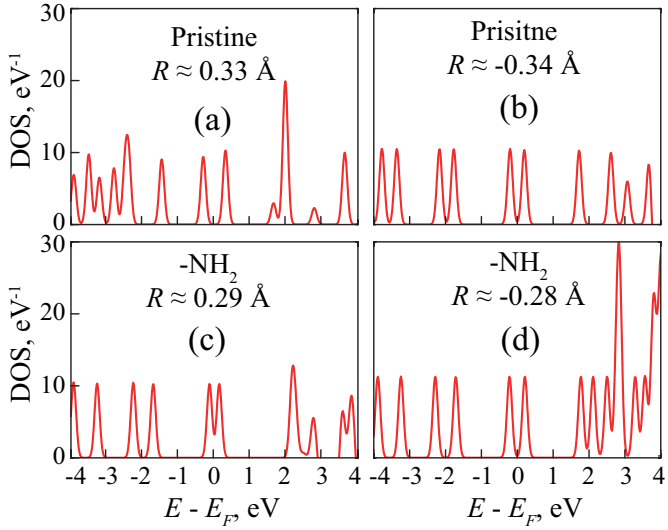


Figure S9: DFTB calculated $p$-orbital DOS of (a, b) pristine CB and (c, d) CB with -$NH_2$ side groups in geometries corresponding to two local minima of the total energy.

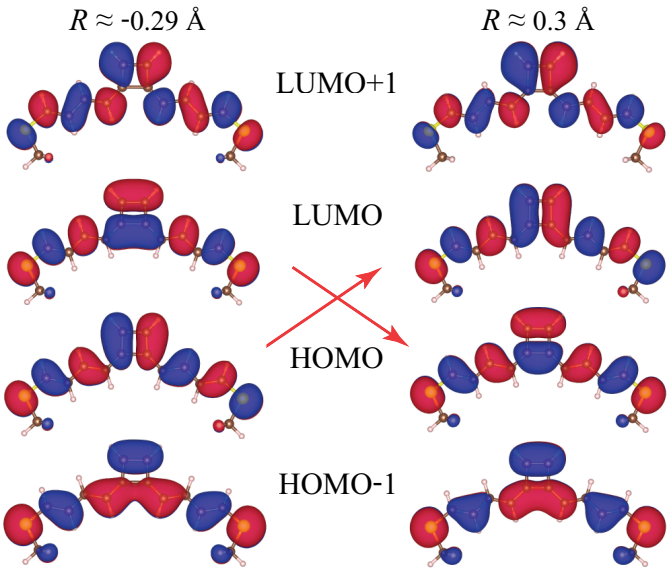


Figure S10: DFT calculated frontier orbitals of pristine CB in geometries corresponding to two local minima of the total energy.

## S4 AR coalescence in cyclobutadiene with different side groups

We carried out the DFTB simulations of CB with different side groups, including -$CH_3$, -OH, -SH, and polyenes. The dependence of the characteristic parameter $R$ [defined in Eq. (21) of the main text] in optimal geometry on the side group is presented in Figure S7. Optimized geometries of -H, -$CH_3$ and polyenes with an even number of carbon atoms have $R > 0$ and thus demonstrate two ARs in the transmisison spectrum. Other side groups lead to the optimal geometry with $R < 0$ and no DQI takes place. Energy-dependent transmission coefficients for -$CH_3$, and two polyene side chains are shown in Figure S8. The behavior is similar to observed in pristine CB and CB with -$NH_2$ side groups or mechanically stretched molecule.

It should be noted, that DFTB structural optimization for CB with -H, -$CH_3$, and -$NH_2$ groups gives two local minima of the total energy (with double bonds of the CB cycle oriented parallel or normal to the current flow direction). Figure S7 shows the global minimum for each of these side groups. On the other hand, DFTB optimization for the rest of the side groups gives a single minimum of the total energy (regardless the starting geometry). We attribute this effect to different charge transfer from the side groups, which affects the carbon atoms' self-energy in CB.

Figure S9 depicts DFTB calculated DOS spectra. The peaks positions drastically change when the geometry of the molecule transforms from one local minimum of the total energy to another. MOs calculated via DFT are similar to DFTB results (Figure 7a of the main text) and the switching of HOMO and LUMO is observed here too (Figure S10).

## S5 Fitting DFTB simulations of CB by Hückel model

We fitted DFTB transport calculations of pristine CB and with -$NH_2$ side groups, performed in the main text, by a simple Hückel model (see Fig. S11). Hopping matrix elements $\tau_{ij}$ between $2p_z$-orbitals of carbon atoms in $sp^2$ hybridization were extracted from some additional *ab initio* calculation.

In the optimized geometry of the molecule we have determined the distances $d_{ij}$ between each pair of carbon atoms being next-nearest neighbors. Then an ethylene molecule (dimer with carbon atoms in $sp^2$ hybridization) was simulated with fixed distance between carbon atoms equal to $d_{ij}$, and the hopping $\tau_{ij}$ was determined as a half gap between HOMO and LUMO of this auxiliary ethylene molecule. Values of $\tau_{ij}$ are presented in Table S1. We also assume that different groups affect not only the geometry of the chemical bonds in the cycle, but also effective on-site energies of the atoms they are attached to. Thus, we additionally introduce some energy shift $\Delta$, which we

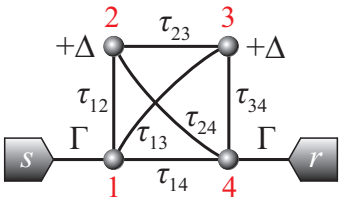


Figure S11: Hückel models for fitting DFTB calculate transmission spectra of CB with -H and -$NH_2$ groups.

Table S1: Hückel hopping matrix elements $\tau_{ij}$ (in eV).

| ligand group, $R$ | $\tau_{12}$ | $\tau_{13}$ | $\tau_{14}$ | $\tau_{23}$ | $\tau_{24}$ | $\tau_{34}$ |
|---|---|---|---|---|---|---|
| -H, $R = 0.33$ Å | 1.8750 | 0.6225 | 2.4870 | 2.8705 | 0.6225 | 1.8750 |
| -H, $R = -0.34$ Å | 2.6345 | 0.6230 | 1.6825 | 2.1395 | 0.6230 | 2.6345 |
| -$NH_2$, $R = 0.29$ Å | 1.9555 | 0.6240 | 2.4240 | 2.7070 | 0.6240 | 1.9555 |
| -$NH_2$, $R = -0.28$ Å | 2.5520 | 0.6195 | 1.7495 | 2.1280 | 0.6195 | 2.5520 |

set $\Delta = 0$ for pristine CB and $\Delta = -0.23$ eV for -$NH_2$ side groups [S19].

## S6 BIC in benzene with electrodes in para-configuration

DFT calculations of DOS spectra for benzene in para-configuration are shown in Figure S12. Additionally, in Figure S13, we plot MOs for isolated benzene molecule, benzene with polyene spacers and anchor groups in para-configuration, and para-benzene between gold electrodes to show that BICs remain localized after attachment to electrodes and other energy levels, for example, HOMO and LUMO, spread electron density to the contacts, i.e., interact with them.

We observe ARs in the transmission spectrum (see Figure S14) of para-benzene with -$NH_2$ side groups connected to the carbon atoms from one side of the molecule (atoms 2 and 3 in Figure 5a from the main text) and in crossed-positions (atoms 2 and 5). No DQI were observed for benzene with four side groups around (atoms 2, 3, 5, and 6) and groups located on the left (atoms 2 and 6) and right (atoms 3 and 5) sides of the ring. For –OH, -SH, and -$CH_3$ groups, the effect is reproduced.

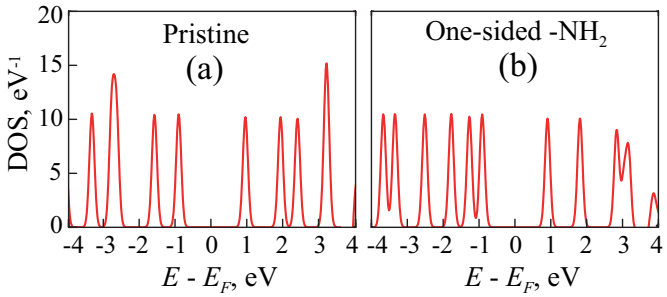


Figure S12: DFTB calculated $p$-orbital DOS of (a) pristine benzene and (b) benzene with -$NH_2$ side groups from one side (atoms 2 and 3 in Figure 5a from the main text). In both cases polyene spacers and anchor groups are included.

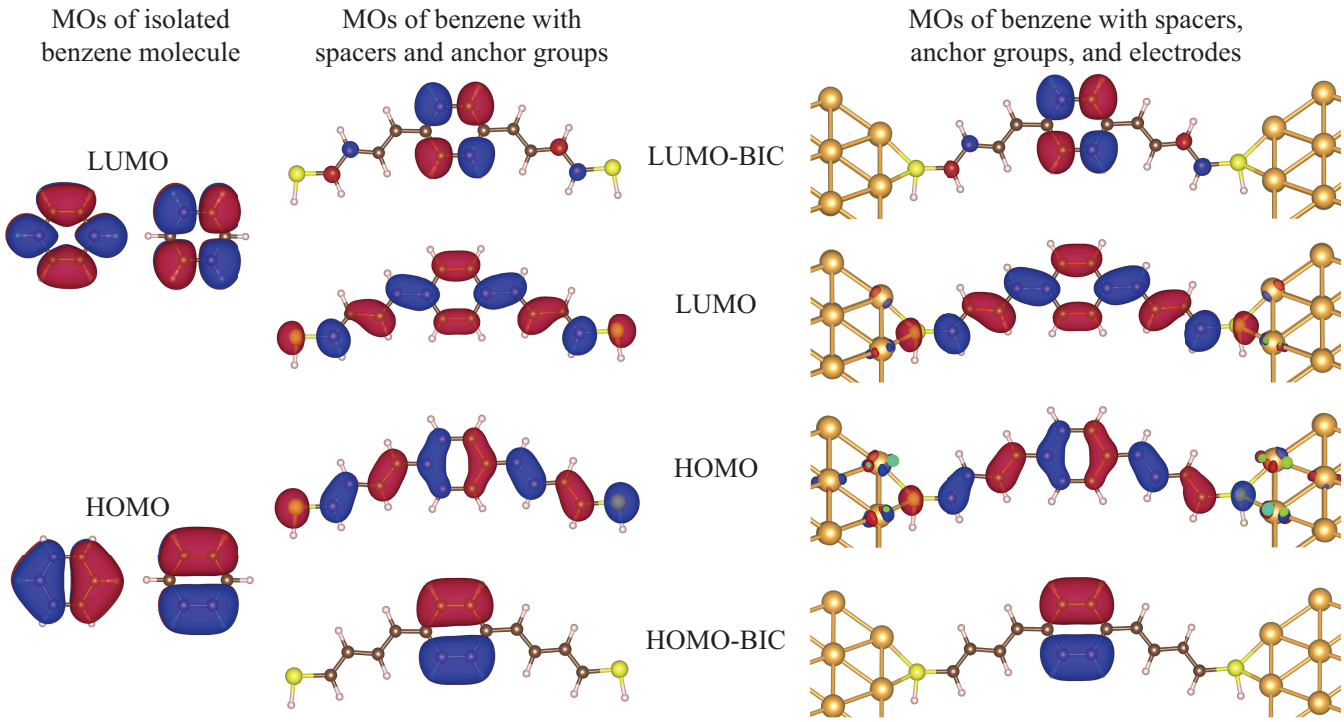


Figure S13: DFT calculated MOs of the isolated benzne molecule, benzene with spacers and anchor groups, and benzene with electrodes in para-configuration. BICs are localized in the benzene cycle, whereas ordinary orbitals (e.g., HOMO and LUMO of the benzene with polyenes and spacers) are delocalized and spread well into electrodes.

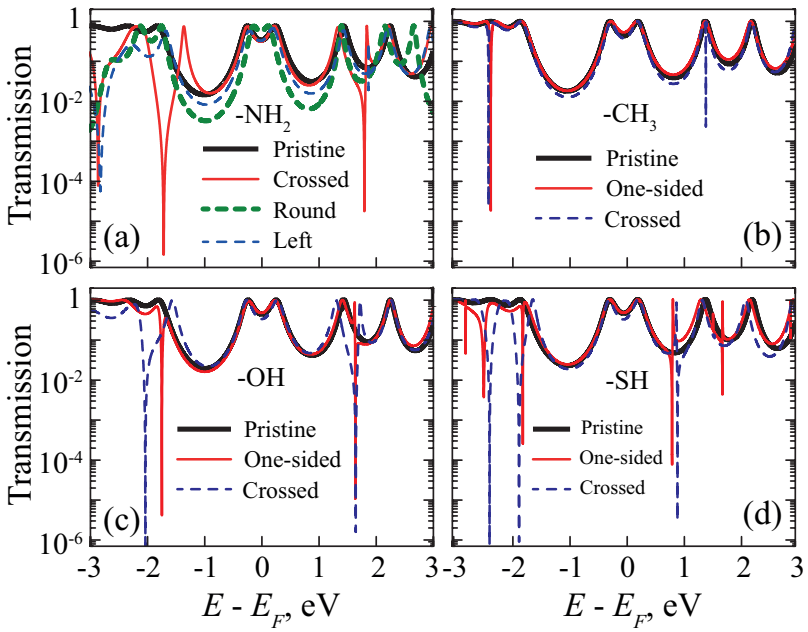


Figure S14: DFTB calculated transmission coefficient spectra of benzene with (a) -$NH_2$, (b) -$CH_3$, (c) -OH, and (d) -SH side groups in different configurations.

# S7 Details on DFT simulations

The optimized geometries of scattering region of CB and benzene with polyene spacers, anchor groups, and gold electrodes used in DFT calculations are presented below.

## S7.1 Pristine cyclobutadiene, $R = -0.29$ Å

```
104
Central region: Cartesian (Angstrom) / fractional
Au   -1.100000e+00  2.300000e+00  1.177247e+00    0.02637  0.23000  0.03514
Au    1.783758e+00  2.300000e+00  1.177247e+00    0.38684  0.23000  0.03514
Au    4.667516e+00  2.300000e+00  1.177247e+00    0.74731  0.23000  0.03514
Au   -2.541879e+00  4.797408e+00  1.177247e+00    0.02408  0.47974  0.03514
Au    3.418791e-01  4.797408e+00  1.177247e+00    0.38455  0.47974  0.03514
Au    3.225637e+00  4.797408e+00  1.177247e+00    0.74502  0.47974  0.03514
Au   -3.983758e+00  7.294816e+00  1.177247e+00    0.02179  0.72948  0.03514
Au   -1.100000e+00  7.294816e+00  1.177247e+00    0.38226  0.72948  0.03514
Au    1.783758e+00  7.294816e+00  1.177247e+00    0.74273  0.72948  0.03514
Au    3.418791e-01  3.132469e+00  3.531826e+00    0.26592  0.31325  0.10542
Au    3.225637e+00  3.132469e+00  3.531826e+00    0.62639  0.31325  0.10542
Au    6.109396e+00  3.132469e+00  3.531826e+00    0.98686  0.31325  0.10542
Au   -1.100000e+00  5.629877e+00  3.531826e+00    0.26363  0.56299  0.10542
Au    1.783758e+00  5.629877e+00  3.531826e+00    0.62410  0.56299  0.10542
Au    4.667516e+00  5.629877e+00  3.531826e+00    0.98457  0.56299  0.10542
Au   -2.541879e+00  8.127285e+00  3.531826e+00    0.26133  0.81273  0.10542
Au    3.418791e-01  8.127285e+00  3.531826e+00    0.62180  0.81273  0.10542
Au    3.225637e+00  8.127285e+00  3.531826e+00    0.98227  0.81273  0.10542
Au   -1.100000e+00  3.964939e+00  5.886404e+00    0.14500  0.39649  0.17570
Au    1.783758e+00  3.964939e+00  5.886404e+00    0.50547  0.39649  0.17570
Au    4.667516e+00  3.964939e+00  5.886404e+00    0.86594  0.39649  0.17570
Au   -2.541879e+00  6.462346e+00  5.886404e+00    0.14271  0.64623  0.17570
Au    3.418791e-01  6.462346e+00  5.886404e+00    0.50318  0.64623  0.17570
Au    3.225637e+00  6.462346e+00  5.886404e+00    0.86365  0.64623  0.17570
Au   -3.983758e+00  8.959754e+00  5.886404e+00    0.14041  0.89598  0.17570
Au   -1.100000e+00  8.959754e+00  5.886404e+00    0.50088  0.89598  0.17570
Au    1.783758e+00  8.959754e+00  5.886404e+00    0.86135  0.89598  0.17570
Au   -1.100000e+00  2.300000e+00  8.240983e+00    0.02637  0.23000  0.24598
Au    1.783758e+00  2.300000e+00  8.240983e+00    0.38684  0.23000  0.24598
Au    4.667516e+00  2.300000e+00  8.240983e+00    0.74731  0.23000  0.24598
Au   -2.541879e+00  4.797408e+00  8.240983e+00    0.02408  0.47974  0.24598
Au    3.418791e-01  4.797408e+00  8.240983e+00    0.38455  0.47974  0.24598
Au    3.225637e+00  4.797408e+00  8.240983e+00    0.74502  0.47974  0.24598
Au   -3.983758e+00  7.294816e+00  8.240983e+00    0.02179  0.72948  0.24598
Au   -1.100000e+00  7.294816e+00  8.240983e+00    0.38226  0.72948  0.24598
Au    1.783758e+00  7.294816e+00  8.240983e+00    0.74273  0.72948  0.24598
S     3.383564e-01  3.139835e+00  9.939650e+00    0.26601  0.31398  0.29668
H     4.269698e-01  7.785463e-01  9.986198e+00    0.10884  0.07785  0.29807
C     3.979296e-01  1.540463e+00  1.077396e+01    0.15950  0.15405  0.32158
H     2.789271e-01  5.294785e+00  1.088718e+01    0.41212  0.52948  0.32496
C     2.910826e-01  4.262937e+00  1.125010e+01    0.34012  0.42629  0.33580
H     1.302709e+00  1.457255e+00  1.138996e+01    0.26667  0.14573  0.33997
H    -4.967159e-01  1.384738e+00  1.139012e+01    0.03657  0.13847  0.33998
C     2.709078e-01  4.017716e+00  1.260152e+01    0.32013  0.40177  0.37613
H     2.924450e-01  2.984989e+00  1.295883e+01    0.24924  0.29850  0.38680
H     1.766677e-01  6.075488e+00  1.320588e+01    0.45496  0.60755  0.39417
```

| | | | | | | |
|---|---|---|---|---|---|---|
| C | 2.245215e-01 | 5.046500e+00 | 1.357742e+01 | 0.38763 | 0.50465 | 0.40526 |
| C | 2.355752e-01 | 4.839287e+00 | 1.495061e+01 | 0.37425 | 0.48393 | 0.44625 |
| H | 1.488476e-01 | 8.018263e+00 | 1.522952e+01 | 0.58991 | 0.80183 | 0.45458 |
| H | 2.781985e-01 | 3.803024e+00 | 1.530271e+01 | 0.30574 | 0.38030 | 0.45676 |
| C | 2.054028e-01 | 5.845157e+00 | 1.592826e+01 | 0.44214 | 0.58452 | 0.47543 |
| C | 1.669320e-01 | 7.231580e+00 | 1.598111e+01 | 0.53612 | 0.72316 | 0.47701 |
| C | 1.668427e-01 | 7.240623e+00 | 1.745338e+01 | 0.53675 | 0.72406 | 0.52095 |
| C | 2.055761e-01 | 5.855175e+00 | 1.752271e+01 | 0.44288 | 0.58552 | 0.52302 |
| H | 2.812631e-01 | 3.820402e+00 | 1.816771e+01 | 0.30736 | 0.38204 | 0.54228 |
| H | 1.494298e-01 | 8.037611e+00 | 1.819466e+01 | 0.59136 | 0.80376 | 0.54308 |
| C | 2.335710e-01 | 4.858672e+00 | 1.850952e+01 | 0.37538 | 0.48587 | 0.55248 |
| C | 2.058908e-01 | 5.075841e+00 | 1.988047e+01 | 0.38739 | 0.50758 | 0.59340 |
| H | 1.525524e-01 | 6.107489e+00 | 2.024244e+01 | 0.45423 | 0.61075 | 0.60420 |
| H | 2.897344e-01 | 3.019690e+00 | 2.052238e+01 | 0.25137 | 0.30197 | 0.61256 |
| C | 2.376449e-01 | 4.055930e+00 | 2.086580e+01 | 0.31869 | 0.40559 | 0.62281 |
| H | 1.197044e+00 | 1.506115e+00 | 2.213578e+01 | 0.25694 | 0.15061 | 0.66072 |
| H | -6.009878e-01 | 1.438618e+00 | 2.213958e+01 | 0.02738 | 0.14386 | 0.66083 |
| C | 2.064323e-01 | 4.320346e+00 | 2.221240e+01 | 0.33363 | 0.43203 | 0.66300 |
| H | 1.546934e-01 | 5.356310e+00 | 2.255493e+01 | 0.40097 | 0.53563 | 0.67323 |
| C | 2.943756e-01 | 1.609578e+00 | 2.275179e+01 | 0.15148 | 0.16096 | 0.67910 |
| S | 2.495279e-01 | 3.264475e+00 | 2.355172e+01 | 0.26378 | 0.32645 | 0.70298 |
| H | 3.203443e-01 | 8.765713e-01 | 2.356665e+01 | 0.10250 | 0.08766 | 0.70343 |
| Au | -1.192351e+00 | 2.432006e+00 | 2.526172e+01 | 0.02424 | 0.24320 | 0.75402 |
| Au | 1.691407e+00 | 2.432006e+00 | 2.526172e+01 | 0.38471 | 0.24320 | 0.75402 |
| Au | 4.575165e+00 | 2.432006e+00 | 2.526172e+01 | 0.74518 | 0.24320 | 0.75402 |
| Au | -2.634230e+00 | 4.929414e+00 | 2.526172e+01 | 0.02194 | 0.49294 | 0.75402 |
| Au | 2.495279e-01 | 4.929414e+00 | 2.526172e+01 | 0.38241 | 0.49294 | 0.75402 |
| Au | 3.133286e+00 | 4.929414e+00 | 2.526172e+01 | 0.74288 | 0.49294 | 0.75402 |
| Au | -4.076109e+00 | 7.426822e+00 | 2.526172e+01 | 0.01965 | 0.74268 | 0.75402 |
| Au | -1.192351e+00 | 7.426822e+00 | 2.526172e+01 | 0.38012 | 0.74268 | 0.75402 |
| Au | 1.691407e+00 | 7.426822e+00 | 2.526172e+01 | 0.74059 | 0.74268 | 0.75402 |
| Au | -1.192351e+00 | 4.096944e+00 | 2.761630e+01 | 0.14286 | 0.40969 | 0.82430 |
| Au | 1.691407e+00 | 4.096944e+00 | 2.761630e+01 | 0.50333 | 0.40969 | 0.82430 |
| Au | 4.575165e+00 | 4.096944e+00 | 2.761630e+01 | 0.86380 | 0.40969 | 0.82430 |
| Au | -2.634230e+00 | 6.594352e+00 | 2.761630e+01 | 0.14057 | 0.65944 | 0.82430 |
| Au | 2.495279e-01 | 6.594352e+00 | 2.761630e+01 | 0.50104 | 0.65944 | 0.82430 |
| Au | 3.133286e+00 | 6.594352e+00 | 2.761630e+01 | 0.86151 | 0.65944 | 0.82430 |
| Au | -4.076109e+00 | 9.091760e+00 | 2.761630e+01 | 0.13827 | 0.90918 | 0.82430 |
| Au | -1.192351e+00 | 9.091760e+00 | 2.761630e+01 | 0.49874 | 0.90918 | 0.82430 |
| Au | 1.691407e+00 | 9.091760e+00 | 2.761630e+01 | 0.85921 | 0.90918 | 0.82430 |
| Au | 2.495279e-01 | 3.264475e+00 | 2.997088e+01 | 0.26378 | 0.32645 | 0.89458 |
| Au | 3.133286e+00 | 3.264475e+00 | 2.997088e+01 | 0.62425 | 0.32645 | 0.89458 |
| Au | 6.017044e+00 | 3.264475e+00 | 2.997088e+01 | 0.98472 | 0.32645 | 0.89458 |
| Au | -1.192351e+00 | 5.761883e+00 | 2.997088e+01 | 0.26149 | 0.57619 | 0.89458 |
| Au | 1.691407e+00 | 5.761883e+00 | 2.997088e+01 | 0.62196 | 0.57619 | 0.89458 |
| Au | 4.575165e+00 | 5.761883e+00 | 2.997088e+01 | 0.98243 | 0.57619 | 0.89458 |
| Au | -2.634230e+00 | 8.259291e+00 | 2.997088e+01 | 0.25920 | 0.82593 | 0.89458 |
| Au | 2.495279e-01 | 8.259291e+00 | 2.997088e+01 | 0.61967 | 0.82593 | 0.89458 |
| Au | 3.133286e+00 | 8.259291e+00 | 2.997088e+01 | 0.98014 | 0.82593 | 0.89458 |
| Au | -1.192351e+00 | 2.432006e+00 | 3.232546e+01 | 0.02424 | 0.24320 | 0.96486 |
| Au | 1.691407e+00 | 2.432006e+00 | 3.232546e+01 | 0.38471 | 0.24320 | 0.96486 |
| Au | 4.575165e+00 | 2.432006e+00 | 3.232546e+01 | 0.74518 | 0.24320 | 0.96486 |
| Au | -2.634230e+00 | 4.929414e+00 | 3.232546e+01 | 0.02194 | 0.49294 | 0.96486 |
| Au | 2.495279e-01 | 4.929414e+00 | 3.232546e+01 | 0.38241 | 0.49294 | 0.96486 |

```
Au    3.133286e+00  4.929414e+00  3.232546e+01    0.74288  0.49294  0.96486
Au   -4.076109e+00  7.426822e+00  3.232546e+01    0.01965  0.74268  0.96486
Au   -1.192351e+00  7.426822e+00  3.232546e+01    0.38012  0.74268  0.96486
Au    1.691407e+00  7.426822e+00  3.232546e+01    0.74059  0.74268  0.96486
```

### S7.2 Pristine cyclobutadiene, $R = 0.3$ Å

```
104
Central region: Cartesian (Angstrom) / fractional
Au    1.108630e-01  4.052819e-01  1.247647e+00    0.03630  0.04057  0.03722
Au    2.994621e+00  4.052819e-01  1.247647e+00    0.33985  0.04057  0.03722
Au    5.878379e+00  4.052819e-01  1.247647e+00    0.64341  0.04057  0.03722
Au   -1.331016e+00  2.902690e+00  1.247647e+00    0.03630  0.29057  0.03722
Au    1.552742e+00  2.902690e+00  1.247647e+00    0.33985  0.29057  0.03722
Au    4.436500e+00  2.902690e+00  1.247647e+00    0.64341  0.29057  0.03722
Au   -2.772895e+00  5.400098e+00  1.247647e+00    0.03630  0.54057  0.03722
Au    1.108630e-01  5.400098e+00  1.247647e+00    0.33985  0.54057  0.03722
Au    2.994621e+00  5.400098e+00  1.247647e+00    0.64341  0.54057  0.03722
Au    1.552742e+00  1.237751e+00  3.602226e+00    0.23867  0.12390  0.10747
Au    4.436500e+00  1.237751e+00  3.602226e+00    0.54222  0.12390  0.10747
Au    7.320259e+00  1.237751e+00  3.602226e+00    0.84578  0.12390  0.10747
Au    1.108630e-01  3.735159e+00  3.602226e+00    0.23867  0.37390  0.10747
Au    2.994621e+00  3.735159e+00  3.602226e+00    0.54222  0.37390  0.10747
Au    5.878379e+00  3.735159e+00  3.602226e+00    0.84578  0.37390  0.10747
Au   -1.331016e+00  6.232567e+00  3.602226e+00    0.23867  0.62390  0.10747
Au    1.552742e+00  6.232567e+00  3.602226e+00    0.54222  0.62390  0.10747
Au    4.436500e+00  6.232567e+00  3.602226e+00    0.84578  0.62390  0.10747
Au    1.108630e-01  2.070220e+00  5.956804e+00    0.13748  0.20724  0.17771
Au    2.994621e+00  2.070220e+00  5.956804e+00    0.44104  0.20724  0.17771
Au    5.878379e+00  2.070220e+00  5.956804e+00    0.74459  0.20724  0.17771
Au   -1.331016e+00  4.567628e+00  5.956804e+00    0.13748  0.45724  0.17771
Au    1.552742e+00  4.567628e+00  5.956804e+00    0.44104  0.45724  0.17771
Au    4.436500e+00  4.567628e+00  5.956804e+00    0.74459  0.45724  0.17771
Au   -2.772895e+00  7.065036e+00  5.956804e+00    0.13749  0.70724  0.17771
Au    1.108630e-01  7.065036e+00  5.956804e+00    0.44104  0.70724  0.17771
Au    2.994621e+00  7.065036e+00  5.956804e+00    0.74459  0.70724  0.17771
Au    1.108630e-01  4.052819e-01  8.311383e+00    0.03630  0.04057  0.24796
Au    2.994621e+00  4.052819e-01  8.311383e+00    0.33985  0.04057  0.24796
Au    5.878379e+00  4.052819e-01  8.311383e+00    0.64341  0.04057  0.24796
Au   -1.331016e+00  2.902690e+00  8.311383e+00    0.03630  0.29057  0.24796
Au    1.552742e+00  2.902690e+00  8.311383e+00    0.33985  0.29057  0.24796
Au    4.436500e+00  2.902690e+00  8.311383e+00    0.64341  0.29057  0.24796
Au   -2.772895e+00  5.400098e+00  8.311383e+00    0.03630  0.54057  0.24796
Au    1.108630e-01  5.400098e+00  8.311383e+00    0.33985  0.54057  0.24796
Au    2.994621e+00  5.400098e+00  8.311383e+00    0.64341  0.54057  0.24796
H     2.937887e+00  1.386063e+00  9.965722e+00    0.39349  0.13875  0.29731
S     2.974887e+00  3.755063e+00  1.000272e+01    0.54136  0.37590  0.29841
C     2.942887e+00  2.124063e+00  1.079172e+01    0.43886  0.21263  0.32195
H     3.009887e+00  5.890063e+00  1.100672e+01    0.67479  0.58962  0.32837
C     2.987887e+00  4.844063e+00  1.135272e+01    0.60891  0.48491  0.33869
H     2.027887e+00  2.001063e+00  1.140472e+01    0.33507  0.20031  0.34024
H     3.844887e+00  1.969063e+00  1.141672e+01    0.52439  0.19711  0.34060
C     2.974887e+00  4.564063e+00  1.269572e+01    0.59052  0.45688  0.37875
```

| | | | | | | |
|---|---|---|---|---|---|---|
| H | 2.952887e+00 | 3.515063e+00 | 1.302672e+01 | 0.52445 | 0.35187 | 0.38863 |
| H | 3.003887e+00 | 6.615063e+00 | 1.339472e+01 | 0.71822 | 0.66219 | 0.39961 |
| C | 2.986887e+00 | 5.560063e+00 | 1.371272e+01 | 0.65232 | 0.55658 | 0.40909 |
| C | 2.970887e+00 | 5.281063e+00 | 1.507472e+01 | 0.63368 | 0.52865 | 0.44973 |
| H | 3.072887e+00 | 8.560063e+00 | 1.534172e+01 | 0.84369 | 0.85689 | 0.45769 |
| H | 2.946887e+00 | 4.226063e+00 | 1.539072e+01 | 0.56703 | 0.42305 | 0.45915 |
| C | 2.981887e+00 | 6.245063e+00 | 1.608072e+01 | 0.69342 | 0.62515 | 0.47974 |
| C | 3.029887e+00 | 7.779063e+00 | 1.610872e+01 | 0.79170 | 0.77871 | 0.48057 |
| C | 3.004887e+00 | 7.779063e+00 | 1.746672e+01 | 0.78907 | 0.77871 | 0.52109 |
| C | 2.954887e+00 | 6.245063e+00 | 1.749272e+01 | 0.69058 | 0.62515 | 0.52186 |
| H | 2.854887e+00 | 4.228063e+00 | 1.818372e+01 | 0.55747 | 0.42325 | 0.54248 |
| H | 3.010887e+00 | 8.560063e+00 | 1.823372e+01 | 0.83716 | 0.85689 | 0.54397 |
| C | 2.900887e+00 | 5.282063e+00 | 1.849972e+01 | 0.62637 | 0.52875 | 0.55191 |
| C | 2.897887e+00 | 5.562063e+00 | 1.986072e+01 | 0.64307 | 0.55678 | 0.59251 |
| H | 2.941887e+00 | 6.616063e+00 | 2.017972e+01 | 0.71176 | 0.66229 | 0.60203 |
| H | 2.821887e+00 | 3.518063e+00 | 2.054572e+01 | 0.51085 | 0.35217 | 0.61294 |
| C | 2.845887e+00 | 4.566063e+00 | 2.087772e+01 | 0.57706 | 0.45708 | 0.62285 |
| H | 1.815887e+00 | 2.008063e+00 | 2.216272e+01 | 0.31318 | 0.20101 | 0.66118 |
| H | 3.632887e+00 | 1.956063e+00 | 2.216572e+01 | 0.50129 | 0.19581 | 0.66127 |
| C | 2.828887e+00 | 4.846063e+00 | 2.222172e+01 | 0.59229 | 0.48511 | 0.66295 |
| H | 2.848887e+00 | 5.891063e+00 | 2.256772e+01 | 0.65790 | 0.58972 | 0.67327 |
| C | 2.727887e+00 | 2.124063e+00 | 2.278172e+01 | 0.41623 | 0.21263 | 0.67965 |
| S | 2.772887e+00 | 3.757063e+00 | 2.356872e+01 | 0.52021 | 0.37610 | 0.70313 |
| H | 2.705887e+00 | 1.388063e+00 | 2.360972e+01 | 0.36919 | 0.13895 | 0.70435 |
| Au | -1.108712e-01 | 4.271859e-01 | 2.527872e+01 | 0.01429 | 0.04276 | 0.75415 |
| Au | 2.772887e+00 | 4.271859e-01 | 2.527872e+01 | 0.31784 | 0.04276 | 0.75415 |
| Au | 5.656645e+00 | 4.271859e-01 | 2.527872e+01 | 0.62140 | 0.04276 | 0.75415 |
| Au | -1.552750e+00 | 2.924594e+00 | 2.527872e+01 | 0.01429 | 0.29276 | 0.75415 |
| Au | 1.331008e+00 | 2.924594e+00 | 2.527872e+01 | 0.31784 | 0.29276 | 0.75415 |
| Au | 4.214766e+00 | 2.924594e+00 | 2.527872e+01 | 0.62140 | 0.29276 | 0.75415 |
| Au | -2.994629e+00 | 5.422002e+00 | 2.527872e+01 | 0.01429 | 0.54276 | 0.75415 |
| Au | -1.108712e-01 | 5.422002e+00 | 2.527872e+01 | 0.31784 | 0.54276 | 0.75415 |
| Au | 2.772887e+00 | 5.422002e+00 | 2.527872e+01 | 0.62140 | 0.54276 | 0.75415 |
| Au | -1.108712e-01 | 2.092124e+00 | 2.763330e+01 | 0.11548 | 0.20943 | 0.82439 |
| Au | 2.772887e+00 | 2.092124e+00 | 2.763330e+01 | 0.41903 | 0.20943 | 0.82439 |
| Au | 5.656645e+00 | 2.092124e+00 | 2.763330e+01 | 0.72258 | 0.20943 | 0.82439 |
| Au | -1.552750e+00 | 4.589532e+00 | 2.763330e+01 | 0.11548 | 0.45943 | 0.82439 |
| Au | 1.331008e+00 | 4.589532e+00 | 2.763330e+01 | 0.41903 | 0.45943 | 0.82439 |
| Au | 4.214766e+00 | 4.589532e+00 | 2.763330e+01 | 0.72258 | 0.45943 | 0.82439 |
| Au | -2.994629e+00 | 7.086940e+00 | 2.763330e+01 | 0.11548 | 0.70943 | 0.82439 |
| Au | -1.108712e-01 | 7.086940e+00 | 2.763330e+01 | 0.41903 | 0.70943 | 0.82439 |
| Au | 2.772887e+00 | 7.086940e+00 | 2.763330e+01 | 0.72258 | 0.70943 | 0.82439 |
| Au | 1.331008e+00 | 1.259655e+00 | 2.998788e+01 | 0.21666 | 0.12610 | 0.89463 |
| Au | 4.214766e+00 | 1.259655e+00 | 2.998788e+01 | 0.52021 | 0.12610 | 0.89463 |
| Au | 7.098524e+00 | 1.259655e+00 | 2.998788e+01 | 0.82377 | 0.12610 | 0.89463 |
| Au | -1.108712e-01 | 3.757063e+00 | 2.998788e+01 | 0.21666 | 0.37610 | 0.89463 |
| Au | 2.772887e+00 | 3.757063e+00 | 2.998788e+01 | 0.52021 | 0.37610 | 0.89463 |
| Au | 5.656645e+00 | 3.757063e+00 | 2.998788e+01 | 0.82377 | 0.37610 | 0.89463 |
| Au | -1.552750e+00 | 6.254471e+00 | 2.998788e+01 | 0.21666 | 0.62610 | 0.89463 |
| Au | 1.331008e+00 | 6.254471e+00 | 2.998788e+01 | 0.52021 | 0.62610 | 0.89463 |
| Au | 4.214766e+00 | 6.254471e+00 | 2.998788e+01 | 0.82377 | 0.62610 | 0.89463 |
| Au | -1.108712e-01 | 4.271859e-01 | 3.234246e+01 | 0.01429 | 0.04276 | 0.96488 |
| Au | 2.772887e+00 | 4.271859e-01 | 3.234246e+01 | 0.31784 | 0.04276 | 0.96488 |
| Au | 5.656645e+00 | 4.271859e-01 | 3.234246e+01 | 0.62140 | 0.04276 | 0.96488 |

```
Au   -1.552750e+00  2.924594e+00  3.234246e+01    0.01429  0.29276  0.96488
Au    1.331008e+00  2.924594e+00  3.234246e+01    0.31784  0.29276  0.96488
Au    4.214766e+00  2.924594e+00  3.234246e+01    0.62140  0.29276  0.96488
Au   -2.994629e+00  5.422002e+00  3.234246e+01    0.01429  0.54276  0.96488
Au   -1.108712e-01  5.422002e+00  3.234246e+01    0.31784  0.54276  0.96488
Au    2.772887e+00  5.422002e+00  3.234246e+01    0.62140  0.54276  0.96488
```

### S7.3 Cyclobutadiene with -$NH_2$ side groups, $R = -0.26$ Å

```
108
Central region: Cartesian (Angstrom) / fractional
Au   -1.100000e+00  2.300000e+00  1.177247e+00    0.02637  0.23000  0.03531
Au    1.783758e+00  2.300000e+00  1.177247e+00    0.38684  0.23000  0.03531
Au    4.667516e+00  2.300000e+00  1.177247e+00    0.74731  0.23000  0.03531
Au   -2.541879e+00  4.797408e+00  1.177247e+00    0.02408  0.47974  0.03531
Au    3.418791e-01  4.797408e+00  1.177247e+00    0.38455  0.47974  0.03531
Au    3.225637e+00  4.797408e+00  1.177247e+00    0.74502  0.47974  0.03531
Au   -3.983758e+00  7.294816e+00  1.177247e+00    0.02179  0.72948  0.03531
Au   -1.100000e+00  7.294816e+00  1.177247e+00    0.38226  0.72948  0.03531
Au    1.783758e+00  7.294816e+00  1.177247e+00    0.74273  0.72948  0.03531
Au    3.418791e-01  3.132469e+00  3.531826e+00    0.26592  0.31325  0.10593
Au    3.225637e+00  3.132469e+00  3.531826e+00    0.62639  0.31325  0.10593
Au    6.109396e+00  3.132469e+00  3.531826e+00    0.98686  0.31325  0.10593
Au   -1.100000e+00  5.629877e+00  3.531826e+00    0.26363  0.56299  0.10593
Au    1.783758e+00  5.629877e+00  3.531826e+00    0.62410  0.56299  0.10593
Au    4.667516e+00  5.629877e+00  3.531826e+00    0.98457  0.56299  0.10593
Au   -2.541879e+00  8.127285e+00  3.531826e+00    0.26133  0.81273  0.10593
Au    3.418791e-01  8.127285e+00  3.531826e+00    0.62180  0.81273  0.10593
Au    3.225637e+00  8.127285e+00  3.531826e+00    0.98227  0.81273  0.10593
Au   -1.100000e+00  3.964939e+00  5.886404e+00    0.14500  0.39649  0.17655
Au    1.783758e+00  3.964939e+00  5.886404e+00    0.50547  0.39649  0.17655
Au    4.667516e+00  3.964939e+00  5.886404e+00    0.86594  0.39649  0.17655
Au   -2.541879e+00  6.462346e+00  5.886404e+00    0.14271  0.64623  0.17655
Au    3.418791e-01  6.462346e+00  5.886404e+00    0.50318  0.64623  0.17655
Au    3.225637e+00  6.462346e+00  5.886404e+00    0.86365  0.64623  0.17655
Au   -3.983758e+00  8.959754e+00  5.886404e+00    0.14041  0.89598  0.17655
Au   -1.100000e+00  8.959754e+00  5.886404e+00    0.50088  0.89598  0.17655
Au    1.783758e+00  8.959754e+00  5.886404e+00    0.86135  0.89598  0.17655
Au   -1.100000e+00  2.300000e+00  8.240983e+00    0.02637  0.23000  0.24716
Au    1.783758e+00  2.300000e+00  8.240983e+00    0.38684  0.23000  0.24716
Au    4.667516e+00  2.300000e+00  8.240983e+00    0.74731  0.23000  0.24716
Au   -2.541879e+00  4.797408e+00  8.240983e+00    0.02408  0.47974  0.24716
Au    3.418791e-01  4.797408e+00  8.240983e+00    0.38455  0.47974  0.24716
Au    3.225637e+00  4.797408e+00  8.240983e+00    0.74502  0.47974  0.24716
Au   -3.983758e+00  7.294816e+00  8.240983e+00    0.02179  0.72948  0.24716
Au   -1.100000e+00  7.294816e+00  8.240983e+00    0.38226  0.72948  0.24716
Au    1.783758e+00  7.294816e+00  8.240983e+00    0.74273  0.72948  0.24716
S     2.478911e-01  3.165772e+00  9.954075e+00    0.25655  0.31658  0.29854
H     1.758806e-01  7.735929e-01  1.014073e+01    0.07710  0.07736  0.30414
H     3.062098e-01  5.415660e+00  1.081337e+01    0.42414  0.54157  0.32432
C     1.913177e-01  1.596676e+00  1.086455e+01    0.13768  0.15967  0.32585
C     2.701812e-01  4.382331e+00  1.118695e+01    0.34601  0.43823  0.33552
H    -7.103202e-01  1.520698e+00  1.148875e+01    0.01956  0.15207  0.34457
```

| | | | | | | |
|---|---|---|---|---|---|---|
| H | 1.071970e+00 | 1.468784e+00 | 1.150985e+01 | 0.23865 | 0.14688 | 0.34520 |
| C | 2.465053e-01 | 4.159794e+00 | 1.254494e+01 | 0.32720 | 0.41598 | 0.37625 |
| H | 2.104537e-01 | 3.131100e+00 | 1.293243e+01 | 0.24940 | 0.31311 | 0.38787 |
| H | 3.030173e-01 | 6.253095e+00 | 1.311084e+01 | 0.48341 | 0.62531 | 0.39322 |
| C | 2.671910e-01 | 5.220683e+00 | 1.349256e+01 | 0.40537 | 0.52207 | 0.40467 |
| H | 1.618645e-01 | 8.172857e+00 | 1.394300e+01 | 0.60255 | 0.81729 | 0.41818 |
| C | 2.423734e-01 | 4.995995e+00 | 1.486343e+01 | 0.38626 | 0.49960 | 0.44578 |
| N | 3.355038e-01 | 8.415391e+00 | 1.492323e+01 | 0.64153 | 0.84154 | 0.44758 |
| H | 1.356491e-01 | 9.379553e+00 | 1.520388e+01 | 0.68525 | 0.93796 | 0.45600 |
| H | 2.121729e-01 | 3.956901e+00 | 1.522472e+01 | 0.30845 | 0.39569 | 0.45662 |
| C | 2.531391e-01 | 6.007999e+00 | 1.583679e+01 | 0.45971 | 0.60080 | 0.47498 |
| C | 2.726240e-01 | 7.424211e+00 | 1.586034e+01 | 0.56305 | 0.74242 | 0.47568 |
| C | 2.768956e-01 | 7.444849e+00 | 1.735629e+01 | 0.56506 | 0.74448 | 0.52055 |
| C | 2.404700e-01 | 6.030166e+00 | 1.741906e+01 | 0.45971 | 0.60302 | 0.52243 |
| H | 4.911766e-01 | 9.410702e+00 | 1.795846e+01 | 0.73191 | 0.94107 | 0.53861 |
| H | 2.008000e-01 | 3.996796e+00 | 1.808770e+01 | 0.30987 | 0.39968 | 0.54249 |
| N | 2.537176e-01 | 8.463285e+00 | 1.826557e+01 | 0.63472 | 0.84633 | 0.54782 |
| C | 2.118115e-01 | 5.045873e+00 | 1.842008e+01 | 0.38599 | 0.50459 | 0.55246 |
| H | 4.180534e-01 | 8.241328e+00 | 1.925227e+01 | 0.63945 | 0.82413 | 0.57742 |
| C | 1.965988e-01 | 5.309226e+00 | 1.978419e+01 | 0.40286 | 0.53092 | 0.59337 |
| H | 2.017199e-01 | 6.352420e+00 | 2.013716e+01 | 0.47782 | 0.63524 | 0.60395 |
| H | 1.711409e-01 | 3.235332e+00 | 2.040192e+01 | 0.25191 | 0.32353 | 0.61190 |
| C | 1.758978e-01 | 4.274965e+00 | 2.076081e+01 | 0.32658 | 0.42750 | 0.62266 |
| H | -7.543782e-01 | 1.648058e+00 | 2.186947e+01 | 0.02313 | 0.16481 | 0.65591 |
| H | 1.028591e+00 | 1.630407e+00 | 2.189020e+01 | 0.24474 | 0.16304 | 0.65653 |
| C | 1.617059e-01 | 4.535702e+00 | 2.211212e+01 | 0.34338 | 0.45357 | 0.66319 |
| H | 1.666642e-01 | 5.579578e+00 | 2.245699e+01 | 0.41838 | 0.55796 | 0.67353 |
| C | 1.309365e-01 | 1.759054e+00 | 2.251150e+01 | 0.14170 | 0.17591 | 0.67517 |
| H | 1.143341e-01 | 9.563595e-01 | 2.325785e+01 | 0.08243 | 0.09564 | 0.69755 |
| S | 1.541783e-01 | 3.349045e+00 | 2.338670e+01 | 0.25789 | 0.33490 | 0.70142 |
| Au | -1.307596e+00 | 2.550043e+00 | 2.510118e+01 | 0.01824 | 0.25500 | 0.75284 |
| Au | 1.576162e+00 | 2.550043e+00 | 2.510118e+01 | 0.37871 | 0.25500 | 0.75284 |
| Au | 4.459921e+00 | 2.550043e+00 | 2.510118e+01 | 0.73918 | 0.25500 | 0.75284 |
| Au | -2.749475e+00 | 5.047451e+00 | 2.510118e+01 | 0.01595 | 0.50475 | 0.75284 |
| Au | 1.342832e-01 | 5.047451e+00 | 2.510118e+01 | 0.37642 | 0.50475 | 0.75284 |
| Au | 3.018041e+00 | 5.047451e+00 | 2.510118e+01 | 0.73689 | 0.50475 | 0.75284 |
| Au | -4.191354e+00 | 7.544859e+00 | 2.510118e+01 | 0.01365 | 0.75449 | 0.75284 |
| Au | -1.307596e+00 | 7.544859e+00 | 2.510118e+01 | 0.37412 | 0.75449 | 0.75284 |
| Au | 1.576162e+00 | 7.544859e+00 | 2.510118e+01 | 0.73459 | 0.75449 | 0.75284 |
| Au | -1.307596e+00 | 4.214982e+00 | 2.745576e+01 | 0.13687 | 0.42150 | 0.82345 |
| Au | 1.576162e+00 | 4.214982e+00 | 2.745576e+01 | 0.49734 | 0.42150 | 0.82345 |
| Au | 4.459921e+00 | 4.214982e+00 | 2.745576e+01 | 0.85781 | 0.42150 | 0.82345 |
| Au | -2.749475e+00 | 6.712390e+00 | 2.745576e+01 | 0.13457 | 0.67124 | 0.82345 |
| Au | 1.342832e-01 | 6.712390e+00 | 2.745576e+01 | 0.49504 | 0.67124 | 0.82345 |
| Au | 3.018041e+00 | 6.712390e+00 | 2.745576e+01 | 0.85551 | 0.67124 | 0.82345 |
| Au | -4.191354e+00 | 9.209798e+00 | 2.745576e+01 | 0.13228 | 0.92098 | 0.82345 |
| Au | -1.307596e+00 | 9.209798e+00 | 2.745576e+01 | 0.49275 | 0.92098 | 0.82345 |
| Au | 1.576162e+00 | 9.209798e+00 | 2.745576e+01 | 0.85322 | 0.92098 | 0.82345 |
| Au | 1.342832e-01 | 3.382513e+00 | 2.981034e+01 | 0.25779 | 0.33825 | 0.89407 |
| Au | 3.018041e+00 | 3.382513e+00 | 2.981034e+01 | 0.61826 | 0.33825 | 0.89407 |
| Au | 5.901800e+00 | 3.382513e+00 | 2.981034e+01 | 0.97873 | 0.33825 | 0.89407 |
| Au | -1.307596e+00 | 5.879920e+00 | 2.981034e+01 | 0.25549 | 0.58799 | 0.89407 |
| Au | 1.576162e+00 | 5.879920e+00 | 2.981034e+01 | 0.61596 | 0.58799 | 0.89407 |
| Au | 4.459921e+00 | 5.879920e+00 | 2.981034e+01 | 0.97643 | 0.58799 | 0.89407 |

```
Au   -2.749475e+00  8.377328e+00  2.981034e+01    0.25320  0.83773  0.89407
Au    1.342832e-01  8.377328e+00  2.981034e+01    0.61367  0.83773  0.89407
Au    3.018041e+00  8.377328e+00  2.981034e+01    0.97414  0.83773  0.89407
Au   -1.307596e+00  2.550043e+00  3.216492e+01    0.01824  0.25500  0.96469
Au    1.576162e+00  2.550043e+00  3.216492e+01    0.37871  0.25500  0.96469
Au    4.459921e+00  2.550043e+00  3.216492e+01    0.73918  0.25500  0.96469
Au   -2.749475e+00  5.047451e+00  3.216492e+01    0.01595  0.50475  0.96469
Au    1.342832e-01  5.047451e+00  3.216492e+01    0.37642  0.50475  0.96469
Au    3.018041e+00  5.047451e+00  3.216492e+01    0.73689  0.50475  0.96469
Au   -4.191354e+00  7.544859e+00  3.216492e+01    0.01365  0.75449  0.96469
Au   -1.307596e+00  7.544859e+00  3.216492e+01    0.37412  0.75449  0.96469
Au    1.576162e+00  7.544859e+00  3.216492e+01    0.73459  0.75449  0.96469
```

### S7.4 Cyclobutadiene with -$NH_2$ side groups, $R = 0.24$ Å

```
108
Central region: Cartesian (Angstrom) / fractional
Au   -1.100000e+00  2.300000e+00  1.177247e+00    0.02637  0.23000  0.03542
Au    1.783758e+00  2.300000e+00  1.177247e+00    0.38684  0.23000  0.03542
Au    4.667516e+00  2.300000e+00  1.177247e+00    0.74731  0.23000  0.03542
Au   -2.541879e+00  4.797408e+00  1.177247e+00    0.02408  0.47974  0.03542
Au    3.418791e-01  4.797408e+00  1.177247e+00    0.38455  0.47974  0.03542
Au    3.225637e+00  4.797408e+00  1.177247e+00    0.74502  0.47974  0.03542
Au   -3.983758e+00  7.294816e+00  1.177247e+00    0.02179  0.72948  0.03542
Au   -1.100000e+00  7.294816e+00  1.177247e+00    0.38226  0.72948  0.03542
Au    1.783758e+00  7.294816e+00  1.177247e+00    0.74273  0.72948  0.03542
Au    3.418791e-01  3.132469e+00  3.531826e+00    0.26592  0.31325  0.10626
Au    3.225637e+00  3.132469e+00  3.531826e+00    0.62639  0.31325  0.10626
Au    6.109396e+00  3.132469e+00  3.531826e+00    0.98686  0.31325  0.10626
Au   -1.100000e+00  5.629877e+00  3.531826e+00    0.26363  0.56299  0.10626
Au    1.783758e+00  5.629877e+00  3.531826e+00    0.62410  0.56299  0.10626
Au    4.667516e+00  5.629877e+00  3.531826e+00    0.98457  0.56299  0.10626
Au   -2.541879e+00  8.127285e+00  3.531826e+00    0.26133  0.81273  0.10626
Au    3.418791e-01  8.127285e+00  3.531826e+00    0.62180  0.81273  0.10626
Au    3.225637e+00  8.127285e+00  3.531826e+00    0.98227  0.81273  0.10626
Au   -1.100000e+00  3.964939e+00  5.886404e+00    0.14500  0.39649  0.17711
Au    1.783758e+00  3.964939e+00  5.886404e+00    0.50547  0.39649  0.17711
Au    4.667516e+00  3.964939e+00  5.886404e+00    0.86594  0.39649  0.17711
Au   -2.541879e+00  6.462346e+00  5.886404e+00    0.14271  0.64623  0.17711
Au    3.418791e-01  6.462346e+00  5.886404e+00    0.50318  0.64623  0.17711
Au    3.225637e+00  6.462346e+00  5.886404e+00    0.86365  0.64623  0.17711
Au   -3.983758e+00  8.959754e+00  5.886404e+00    0.14041  0.89598  0.17711
Au   -1.100000e+00  8.959754e+00  5.886404e+00    0.50088  0.89598  0.17711
Au    1.783758e+00  8.959754e+00  5.886404e+00    0.86135  0.89598  0.17711
Au   -1.100000e+00  2.300000e+00  8.240983e+00    0.02637  0.23000  0.24795
Au    1.783758e+00  2.300000e+00  8.240983e+00    0.38684  0.23000  0.24795
Au    4.667516e+00  2.300000e+00  8.240983e+00    0.74731  0.23000  0.24795
Au   -2.541879e+00  4.797408e+00  8.240983e+00    0.02408  0.47974  0.24795
Au    3.418791e-01  4.797408e+00  8.240983e+00    0.38455  0.47974  0.24795
Au    3.225637e+00  4.797408e+00  8.240983e+00    0.74502  0.47974  0.24795
Au   -3.983758e+00  7.294816e+00  8.240983e+00    0.02179  0.72948  0.24795
Au   -1.100000e+00  7.294816e+00  8.240983e+00    0.38226  0.72948  0.24795
Au    1.783758e+00  7.294816e+00  8.240983e+00    0.74273  0.72948  0.24795
```

| | | | | | | |
|---|---|---|---|---|---|---|
| S | 2.540836e-01 | 3.147958e+00 | 9.938422e+00 | 0.25605 | 0.31480 | 0.29902 |
| H | 3.619368e-01 | 7.911073e-01 | 1.004276e+01 | 0.10161 | 0.07911 | 0.30216 |
| C | 3.147295e-01 | 1.570043e+00 | 1.081301e+01 | 0.15121 | 0.15700 | 0.32534 |
| H | 2.153520e-01 | 5.326389e+00 | 1.083640e+01 | 0.40642 | 0.53264 | 0.32604 |
| C | 2.217626e-01 | 4.304046e+00 | 1.122486e+01 | 0.33438 | 0.43040 | 0.33773 |
| H | -5.867475e-01 | 1.416860e+00 | 1.142037e+01 | 0.02761 | 0.14169 | 0.34361 |
| H | 1.208894e+00 | 1.511070e+00 | 1.144836e+01 | 0.25878 | 0.15111 | 0.34445 |
| C | 2.078188e-01 | 4.083750e+00 | 1.258137e+01 | 0.31694 | 0.40838 | 0.37854 |
| H | 2.099091e-01 | 3.055352e+00 | 1.295134e+01 | 0.24393 | 0.30554 | 0.38967 |
| H | 1.955208e-01 | 6.141265e+00 | 1.318124e+01 | 0.46201 | 0.61413 | 0.39659 |
| C | 1.886761e-01 | 5.113901e+00 | 1.355482e+01 | 0.38795 | 0.51139 | 0.40783 |
| H | -2.376367e-01 | 8.093781e+00 | 1.409005e+01 | 0.54698 | 0.80938 | 0.42393 |
| C | 1.796445e-01 | 4.899453e+00 | 1.493254e+01 | 0.37154 | 0.48995 | 0.44928 |
| N | 1.003578e-01 | 8.383524e+00 | 1.500051e+01 | 0.60987 | 0.83835 | 0.45133 |
| H | -3.153812e-01 | 9.268117e+00 | 1.527799e+01 | 0.62093 | 0.92681 | 0.45968 |
| H | 2.087914e-01 | 3.863613e+00 | 1.528151e+01 | 0.30138 | 0.38636 | 0.45978 |
| C | 1.422348e-01 | 5.878245e+00 | 1.592021e+01 | 0.43660 | 0.58782 | 0.47900 |
| C | 7.830753e-02 | 7.392508e+00 | 1.597129e+01 | 0.53650 | 0.73925 | 0.48054 |
| C | 1.376932e-01 | 5.852623e+00 | 1.734161e+01 | 0.43421 | 0.58526 | 0.52177 |
| C | 9.881223e-02 | 7.369329e+00 | 1.734220e+01 | 0.53742 | 0.73693 | 0.52178 |
| H | 2.116004e-01 | 3.814396e+00 | 1.792019e+01 | 0.29823 | 0.38144 | 0.53917 |
| H | 3.612945e-01 | 9.245451e+00 | 1.809218e+01 | 0.70390 | 0.92455 | 0.54435 |
| C | 1.631446e-01 | 4.840955e+00 | 1.829748e+01 | 0.36531 | 0.48410 | 0.55053 |
| N | 1.561778e-02 | 8.324305e+00 | 1.834496e+01 | 0.59506 | 0.83243 | 0.55195 |
| H | 3.805781e-01 | 8.030377e+00 | 1.924358e+01 | 0.61974 | 0.80304 | 0.57899 |
| C | 1.300086e-01 | 5.017378e+00 | 1.968038e+01 | 0.37374 | 0.50174 | 0.59213 |
| H | 5.881483e-02 | 6.031586e+00 | 2.008223e+01 | 0.43710 | 0.60316 | 0.60423 |
| H | 2.234480e-01 | 2.947249e+00 | 2.023997e+01 | 0.23792 | 0.29472 | 0.60897 |
| C | 1.669758e-01 | 3.966365e+00 | 2.062939e+01 | 0.30348 | 0.39664 | 0.62069 |
| H | 1.144662e+00 | 1.379433e+00 | 2.171924e+01 | 0.24137 | 0.13794 | 0.65348 |
| H | -6.492854e-01 | 1.272322e+00 | 2.174066e+01 | 0.00949 | 0.12723 | 0.65412 |
| C | 1.375148e-01 | 4.160110e+00 | 2.198893e+01 | 0.31360 | 0.41601 | 0.66159 |
| C | 2.500922e-01 | 1.420691e+00 | 2.235410e+01 | 0.13249 | 0.14207 | 0.67258 |
| H | 8.343739e-02 | 5.175788e+00 | 2.239081e+01 | 0.37920 | 0.51758 | 0.67368 |
| H | 3.093243e-01 | 6.320441e-01 | 2.311409e+01 | 0.08370 | 0.06320 | 0.69545 |
| S | 1.744977e-01 | 2.982923e+00 | 2.325525e+01 | 0.23435 | 0.29829 | 0.69969 |
| Au | -1.307596e+00 | 2.232486e+00 | 2.499535e+01 | -0.00438 | 0.22325 | 0.75205 |
| Au | 1.576162e+00 | 2.232486e+00 | 2.499535e+01 | 0.35608 | 0.22325 | 0.75205 |
| Au | 4.459921e+00 | 2.232486e+00 | 2.499535e+01 | 0.71655 | 0.22325 | 0.75205 |
| Au | -2.749475e+00 | 4.729894e+00 | 2.499535e+01 | -0.00668 | 0.47299 | 0.75205 |
| Au | 1.342832e-01 | 4.729894e+00 | 2.499535e+01 | 0.35379 | 0.47299 | 0.75205 |
| Au | 3.018041e+00 | 4.729894e+00 | 2.499535e+01 | 0.71426 | 0.47299 | 0.75205 |
| Au | -4.191354e+00 | 7.227302e+00 | 2.499535e+01 | -0.00897 | 0.72273 | 0.75205 |
| Au | -1.307596e+00 | 7.227302e+00 | 2.499535e+01 | 0.35150 | 0.72273 | 0.75205 |
| Au | 1.576162e+00 | 7.227302e+00 | 2.499535e+01 | 0.71197 | 0.72273 | 0.75205 |
| Au | -1.307596e+00 | 3.897424e+00 | 2.734993e+01 | 0.11424 | 0.38974 | 0.82289 |
| Au | 1.576162e+00 | 3.897424e+00 | 2.734993e+01 | 0.47471 | 0.38974 | 0.82289 |
| Au | 4.459921e+00 | 3.897424e+00 | 2.734993e+01 | 0.83518 | 0.38974 | 0.82289 |
| Au | -2.749475e+00 | 6.394832e+00 | 2.734993e+01 | 0.11195 | 0.63948 | 0.82289 |
| Au | 1.342832e-01 | 6.394832e+00 | 2.734993e+01 | 0.47242 | 0.63948 | 0.82289 |
| Au | 3.018041e+00 | 6.394832e+00 | 2.734993e+01 | 0.83289 | 0.63948 | 0.82289 |
| Au | -4.191354e+00 | 8.892240e+00 | 2.734993e+01 | 0.10965 | 0.88922 | 0.82289 |
| Au | -1.307596e+00 | 8.892240e+00 | 2.734993e+01 | 0.47012 | 0.88922 | 0.82289 |
| Au | 1.576162e+00 | 8.892240e+00 | 2.734993e+01 | 0.83059 | 0.88922 | 0.82289 |

```
Au    1.342832e-01  3.064955e+00  2.970451e+01    0.23516  0.30650  0.89374
Au    3.018041e+00  3.064955e+00  2.970451e+01    0.59563  0.30650  0.89374
Au    5.901800e+00  3.064955e+00  2.970451e+01    0.95610  0.30650  0.89374
Au   -1.307596e+00  5.562363e+00  2.970451e+01    0.23287  0.55624  0.89374
Au    1.576162e+00  5.562363e+00  2.970451e+01    0.59334  0.55624  0.89374
Au    4.459921e+00  5.562363e+00  2.970451e+01    0.95381  0.55624  0.89374
Au   -2.749475e+00  8.059771e+00  2.970451e+01    0.23057  0.80598  0.89374
Au    1.342832e-01  8.059771e+00  2.970451e+01    0.59104  0.80598  0.89374
Au    3.018041e+00  8.059771e+00  2.970451e+01    0.95151  0.80598  0.89374
Au   -1.307596e+00  2.232486e+00  3.205909e+01   -0.00438  0.22325  0.96458
Au    1.576162e+00  2.232486e+00  3.205909e+01    0.35608  0.22325  0.96458
Au    4.459921e+00  2.232486e+00  3.205909e+01    0.71655  0.22325  0.96458
Au   -2.749475e+00  4.729894e+00  3.205909e+01   -0.00668  0.47299  0.96458
Au    1.342832e-01  4.729894e+00  3.205909e+01    0.35379  0.47299  0.96458
Au    3.018041e+00  4.729894e+00  3.205909e+01    0.71426  0.47299  0.96458
Au   -4.191354e+00  7.227302e+00  3.205909e+01   -0.00897  0.72273  0.96458
Au   -1.307596e+00  7.227302e+00  3.205909e+01    0.35150  0.72273  0.96458
Au    1.576162e+00  7.227302e+00  3.205909e+01    0.71197  0.72273  0.96458
```

### S7.5 Pristine benzene in para-configuration

```
102
Central region: Cartesian (Angstrom) / fractional
Au    3.816466e-02  7.221347e-01  1.177247e+00    0.04689  0.08496  0.03325
Au    2.921923e+00  7.221347e-01  1.177247e+00    0.38022  0.08496  0.03325
Au    5.805681e+00  7.221347e-01  1.177247e+00    0.71356  0.08496  0.03325
Au   -1.403714e+00  3.219543e+00  1.177247e+00    0.02713  0.37877  0.03325
Au    1.480044e+00  3.219543e+00  1.177247e+00    0.36046  0.37877  0.03325
Au    4.363802e+00  3.219543e+00  1.177247e+00    0.69380  0.37877  0.03325
Au   -2.845594e+00  5.716950e+00  1.177247e+00    0.00737  0.67258  0.03325
Au    3.816466e-02  5.716950e+00  1.177247e+00    0.34070  0.67258  0.03325
Au    2.921923e+00  5.716950e+00  1.177247e+00    0.67404  0.67258  0.03325
Au    1.480044e+00  1.554604e+00  3.531826e+00    0.26253  0.18289  0.09976
Au    4.363802e+00  1.554604e+00  3.531826e+00    0.59586  0.18289  0.09976
Au    7.247560e+00  1.554604e+00  3.531826e+00    0.92919  0.18289  0.09976
Au    3.816466e-02  4.052012e+00  3.531826e+00    0.24277  0.47671  0.09976
Au    2.921923e+00  4.052012e+00  3.531826e+00    0.57610  0.47671  0.09976
Au    5.805681e+00  4.052012e+00  3.531826e+00    0.90943  0.47671  0.09976
Au   -1.403714e+00  6.549420e+00  3.531826e+00    0.22301  0.77052  0.09976
Au    1.480044e+00  6.549420e+00  3.531826e+00    0.55634  0.77052  0.09976
Au    4.363802e+00  6.549420e+00  3.531826e+00    0.88967  0.77052  0.09976
Au    3.816466e-02  2.387073e+00  5.886404e+00    0.14483  0.28083  0.16626
Au    2.921923e+00  2.387073e+00  5.886404e+00    0.47816  0.28083  0.16626
Au    5.805681e+00  2.387073e+00  5.886404e+00    0.81149  0.28083  0.16626
Au   -1.403714e+00  4.884481e+00  5.886404e+00    0.12507  0.57464  0.16626
Au    1.480044e+00  4.884481e+00  5.886404e+00    0.45840  0.57464  0.16626
Au    4.363802e+00  4.884481e+00  5.886404e+00    0.79173  0.57464  0.16626
Au   -2.845594e+00  7.381889e+00  5.886404e+00    0.10531  0.86846  0.16626
Au    3.816466e-02  7.381889e+00  5.886404e+00    0.43864  0.86846  0.16626
Au    2.921923e+00  7.381889e+00  5.886404e+00    0.77197  0.86846  0.16626
Au    3.816466e-02  7.221347e-01  8.240983e+00    0.04689  0.08496  0.23277
Au    2.921923e+00  7.221347e-01  8.240983e+00    0.38022  0.08496  0.23277
Au    5.805681e+00  7.221347e-01  8.240983e+00    0.71356  0.08496  0.23277
```

| | | | | | | |
|---|---|---|---|---|---|---|
| Au | -1.403714e+00 | 3.219543e+00 | 8.240983e+00 | 0.02713 | 0.37877 | 0.23277 |
| Au | 1.480044e+00 | 3.219543e+00 | 8.240983e+00 | 0.36046 | 0.37877 | 0.23277 |
| Au | 4.363802e+00 | 3.219543e+00 | 8.240983e+00 | 0.69380 | 0.37877 | 0.23277 |
| Au | -2.845594e+00 | 5.716950e+00 | 8.240983e+00 | 0.00737 | 0.67258 | 0.23277 |
| Au | 3.816466e-02 | 5.716950e+00 | 8.240983e+00 | 0.34070 | 0.67258 | 0.23277 |
| Au | 2.921923e+00 | 5.716950e+00 | 8.240983e+00 | 0.67404 | 0.67258 | 0.23277 |
| H | 2.916372e+00 | 2.711601e+00 | 9.700033e+00 | 0.49661 | 0.31901 | 0.27398 |
| S | 2.895266e+00 | 4.055740e+00 | 9.953640e+00 | 0.57324 | 0.47715 | 0.28115 |
| C | 2.883029e+00 | 3.919186e+00 | 1.170253e+01 | 0.56379 | 0.46108 | 0.33054 |
| H | 2.871545e+00 | 6.010283e+00 | 1.209926e+01 | 0.68547 | 0.70709 | 0.34175 |
| H | 2.885272e+00 | 2.899785e+00 | 1.211159e+01 | 0.50408 | 0.34115 | 0.34210 |
| C | 2.871542e+00 | 4.997986e+00 | 1.253375e+01 | 0.62592 | 0.58800 | 0.35402 |
| C | 2.861647e+00 | 4.888652e+00 | 1.396465e+01 | 0.61835 | 0.57514 | 0.39444 |
| H | 2.862671e+00 | 3.865100e+00 | 1.437098e+01 | 0.55826 | 0.45472 | 0.40592 |
| H | 2.849000e+00 | 6.962443e+00 | 1.439356e+01 | 0.73887 | 0.81911 | 0.40655 |
| C | 2.851882e+00 | 5.948935e+00 | 1.482662e+01 | 0.67959 | 0.69987 | 0.41879 |
| C | 2.844311e+00 | 5.890675e+00 | 1.627715e+01 | 0.67528 | 0.69302 | 0.45976 |
| H | 2.866664e+00 | 3.717765e+00 | 1.647174e+01 | 0.55005 | 0.43738 | 0.46525 |
| H | 2.818574e+00 | 8.050192e+00 | 1.650374e+01 | 0.79934 | 0.94708 | 0.46616 |
| C | 2.853368e+00 | 4.674472e+00 | 1.700739e+01 | 0.60479 | 0.54994 | 0.48038 |
| C | 2.827928e+00 | 7.086739e+00 | 1.703331e+01 | 0.74375 | 0.83373 | 0.48112 |
| C | 2.847589e+00 | 4.656581e+00 | 1.839350e+01 | 0.60307 | 0.54783 | 0.51953 |
| C | 2.821577e+00 | 7.068753e+00 | 1.842670e+01 | 0.74196 | 0.83162 | 0.52047 |
| H | 2.855702e+00 | 3.686554e+00 | 1.890529e+01 | 0.54695 | 0.43371 | 0.53399 |
| H | 2.807857e+00 | 8.018567e+00 | 1.897981e+01 | 0.79624 | 0.94336 | 0.53610 |
| C | 2.831981e+00 | 5.854400e+00 | 1.915347e+01 | 0.67173 | 0.68875 | 0.54100 |
| C | 2.827815e+00 | 5.878212e+00 | 2.060496e+01 | 0.67264 | 0.69155 | 0.58200 |
| H | 2.849368e+00 | 3.783138e+00 | 2.103446e+01 | 0.55190 | 0.44508 | 0.59413 |
| H | 2.814402e+00 | 6.881685e+00 | 2.106140e+01 | 0.73012 | 0.80961 | 0.59489 |
| C | 2.838359e+00 | 4.803554e+00 | 2.144890e+01 | 0.61065 | 0.56512 | 0.60584 |
| C | 2.835713e+00 | 4.901262e+00 | 2.288071e+01 | 0.61609 | 0.57662 | 0.64628 |
| H | 2.855176e+00 | 2.800393e+00 | 2.328561e+01 | 0.49476 | 0.32946 | 0.65772 |
| H | 2.823746e+00 | 5.912438e+00 | 2.331924e+01 | 0.67419 | 0.69558 | 0.65867 |
| C | 2.845913e+00 | 3.817537e+00 | 2.370556e+01 | 0.55352 | 0.44912 | 0.66958 |
| S | 2.845586e+00 | 3.779685e+00 | 2.545281e+01 | 0.55126 | 0.44467 | 0.71893 |
| H | 2.834205e+00 | 2.413677e+00 | 2.557194e+01 | 0.46959 | 0.28396 | 0.72229 |
| Au | -3.817201e-02 | 4.498076e-01 | 2.716281e+01 | 0.02205 | 0.05292 | 0.76723 |
| Au | 2.845586e+00 | 4.498076e-01 | 2.716281e+01 | 0.35538 | 0.05292 | 0.76723 |
| Au | 5.729344e+00 | 4.498076e-01 | 2.716281e+01 | 0.68871 | 0.05292 | 0.76723 |
| Au | -1.480051e+00 | 2.947215e+00 | 2.716281e+01 | 0.00229 | 0.34673 | 0.76723 |
| Au | 1.403707e+00 | 2.947215e+00 | 2.716281e+01 | 0.33562 | 0.34673 | 0.76723 |
| Au | 4.287465e+00 | 2.947215e+00 | 2.716281e+01 | 0.66895 | 0.34673 | 0.76723 |
| Au | -2.921930e+00 | 5.444623e+00 | 2.716281e+01 | -0.01747 | 0.64054 | 0.76723 |
| Au | -3.817201e-02 | 5.444623e+00 | 2.716281e+01 | 0.31586 | 0.64054 | 0.76723 |
| Au | 2.845586e+00 | 5.444623e+00 | 2.716281e+01 | 0.64919 | 0.64054 | 0.76723 |
| Au | -3.817201e-02 | 2.114746e+00 | 2.951739e+01 | 0.11998 | 0.24879 | 0.83374 |
| Au | 2.845586e+00 | 2.114746e+00 | 2.951739e+01 | 0.45332 | 0.24879 | 0.83374 |
| Au | 5.729344e+00 | 2.114746e+00 | 2.951739e+01 | 0.78665 | 0.24879 | 0.83374 |
| Au | -1.480051e+00 | 4.612154e+00 | 2.951739e+01 | 0.10022 | 0.54261 | 0.83374 |
| Au | 1.403707e+00 | 4.612154e+00 | 2.951739e+01 | 0.43356 | 0.54261 | 0.83374 |
| Au | 4.287465e+00 | 4.612154e+00 | 2.951739e+01 | 0.76689 | 0.54261 | 0.83374 |
| Au | -2.921930e+00 | 7.109562e+00 | 2.951739e+01 | 0.08046 | 0.83642 | 0.83374 |
| Au | -3.817201e-02 | 7.109562e+00 | 2.951739e+01 | 0.41380 | 0.83642 | 0.83374 |
| Au | 2.845586e+00 | 7.109562e+00 | 2.951739e+01 | 0.74713 | 0.83642 | 0.83374 |

```
Au    1.403707e+00  1.282277e+00  3.187196e+01    0.23768  0.15086  0.90024
Au    4.287465e+00  1.282277e+00  3.187196e+01    0.57102  0.15086  0.90024
Au    7.171224e+00  1.282277e+00  3.187196e+01    0.90435  0.15086  0.90024
Au   -3.817201e-02  3.779685e+00  3.187196e+01    0.21792  0.44467  0.90024
Au    2.845586e+00  3.779685e+00  3.187196e+01    0.55126  0.44467  0.90024
Au    5.729344e+00  3.779685e+00  3.187196e+01    0.88459  0.44467  0.90024
Au   -1.480051e+00  6.277093e+00  3.187196e+01    0.19816  0.73848  0.90024
Au    1.403707e+00  6.277093e+00  3.187196e+01    0.53150  0.73848  0.90024
Au    4.287465e+00  6.277093e+00  3.187196e+01    0.86483  0.73848  0.90024
Au   -3.817201e-02  4.498076e-01  3.422654e+01    0.02205  0.05292  0.96675
Au    2.845586e+00  4.498076e-01  3.422654e+01    0.35538  0.05292  0.96675
Au    5.729344e+00  4.498076e-01  3.422654e+01    0.68871  0.05292  0.96675
Au   -1.480051e+00  2.947215e+00  3.422654e+01    0.00229  0.34673  0.96675
Au    1.403707e+00  2.947215e+00  3.422654e+01    0.33562  0.34673  0.96675
Au    4.287465e+00  2.947215e+00  3.422654e+01    0.66895  0.34673  0.96675
Au   -2.921930e+00  5.444623e+00  3.422654e+01   -0.01747  0.64054  0.96675
Au   -3.817201e-02  5.444623e+00  3.422654e+01    0.31586  0.64054  0.96675
Au    2.845586e+00  5.444623e+00  3.422654e+01    0.64919  0.64054  0.96675
```

### S7.6 Benzene with -$NH_2$ side groups in para-configuration

```
106
Central region: Cartesian (Angstrom) / fractional
Au    3.908897e-02  7.593553e-01  1.177247e+00    0.04326  0.07749  0.03337
Au    2.922847e+00  7.593553e-01  1.177247e+00    0.37659  0.07749  0.03337
Au    5.806605e+00  7.593553e-01  1.177247e+00    0.70993  0.07749  0.03337
Au   -1.402790e+00  3.256763e+00  1.177247e+00    0.00401  0.33232  0.03337
Au    1.480968e+00  3.256763e+00  1.177247e+00    0.33735  0.33232  0.03337
Au    4.364726e+00  3.256763e+00  1.177247e+00    0.67068  0.33232  0.03337
Au   -2.844669e+00  5.754171e+00  1.177247e+00   -0.03523  0.58716  0.03337
Au    3.908897e-02  5.754171e+00  1.177247e+00    0.29810  0.58716  0.03337
Au    2.922847e+00  5.754171e+00  1.177247e+00    0.63143  0.58716  0.03337
Au    1.480968e+00  1.591825e+00  3.531826e+00    0.25240  0.16243  0.10010
Au    4.364726e+00  1.591825e+00  3.531826e+00    0.58573  0.16243  0.10010
Au    7.248485e+00  1.591825e+00  3.531826e+00    0.91907  0.16243  0.10010
Au    3.908897e-02  4.089232e+00  3.531826e+00    0.21315  0.41727  0.10010
Au    2.922847e+00  4.089232e+00  3.531826e+00    0.54649  0.41727  0.10010
Au    5.806605e+00  4.089232e+00  3.531826e+00    0.87982  0.41727  0.10010
Au   -1.402790e+00  6.586640e+00  3.531826e+00    0.17391  0.67211  0.10010
Au    1.480968e+00  6.586640e+00  3.531826e+00    0.50724  0.67211  0.10010
Au    4.364726e+00  6.586640e+00  3.531826e+00    0.84057  0.67211  0.10010
Au    3.908897e-02  2.424294e+00  5.886404e+00    0.12821  0.24738  0.16684
Au    2.922847e+00  2.424294e+00  5.886404e+00    0.46154  0.24738  0.16684
Au    5.806605e+00  2.424294e+00  5.886404e+00    0.79487  0.24738  0.16684
Au   -1.402790e+00  4.921702e+00  5.886404e+00    0.08896  0.50221  0.16684
Au    1.480968e+00  4.921702e+00  5.886404e+00    0.42229  0.50221  0.16684
Au    4.364726e+00  4.921702e+00  5.886404e+00    0.75563  0.50221  0.16684
Au   -2.844669e+00  7.419110e+00  5.886404e+00    0.04971  0.75705  0.16684
Au    3.908897e-02  7.419110e+00  5.886404e+00    0.38304  0.75705  0.16684
Au    2.922847e+00  7.419110e+00  5.886404e+00    0.71638  0.75705  0.16684
Au    3.908897e-02  7.593553e-01  8.240983e+00    0.04326  0.07749  0.23357
Au    2.922847e+00  7.593553e-01  8.240983e+00    0.37659  0.07749  0.23357
Au    5.806605e+00  7.593553e-01  8.240983e+00    0.70993  0.07749  0.23357
```

| | | | | | | |
|---|---|---|---|---|---|---|
| Au | -1.402790e+00 | 3.256763e+00 | 8.240983e+00 | 0.00401 | 0.33232 | 0.23357 |
| Au | 1.480968e+00 | 3.256763e+00 | 8.240983e+00 | 0.33735 | 0.33232 | 0.23357 |
| Au | 4.364726e+00 | 3.256763e+00 | 8.240983e+00 | 0.67068 | 0.33232 | 0.23357 |
| Au | -2.844669e+00 | 5.754171e+00 | 8.240983e+00 | -0.03523 | 0.58716 | 0.23357 |
| Au | 3.908897e-02 | 5.754171e+00 | 8.240983e+00 | 0.29810 | 0.58716 | 0.23357 |
| Au | 2.922847e+00 | 5.754171e+00 | 8.240983e+00 | 0.63143 | 0.58716 | 0.23357 |
| H | 2.918429e+00 | 2.741786e+00 | 9.740965e+00 | 0.47723 | 0.27977 | 0.27608 |
| S | 2.916097e+00 | 4.092395e+00 | 9.957476e+00 | 0.54587 | 0.41759 | 0.28222 |
| C | 2.875251e+00 | 4.003747e+00 | 1.171028e+01 | 0.53662 | 0.40855 | 0.33190 |
| H | 2.798272e+00 | 6.105007e+00 | 1.204097e+01 | 0.63493 | 0.62296 | 0.34127 |
| H | 2.906476e+00 | 2.995844e+00 | 1.214709e+01 | 0.48881 | 0.30570 | 0.34428 |
| C | 2.824787e+00 | 5.107112e+00 | 1.250777e+01 | 0.58708 | 0.52113 | 0.35450 |
| C | 2.812637e+00 | 5.048897e+00 | 1.394050e+01 | 0.58271 | 0.51519 | 0.39511 |
| H | 2.786236e+00 | 7.119403e+00 | 1.424246e+01 | 0.68530 | 0.72647 | 0.40367 |
| H | 2.818534e+00 | 4.040479e+00 | 1.438218e+01 | 0.53194 | 0.41229 | 0.40763 |
| C | 2.800619e+00 | 6.146164e+00 | 1.475844e+01 | 0.63730 | 0.62716 | 0.41829 |
| H | 2.947528e+00 | 8.632126e+00 | 1.533146e+01 | 0.78112 | 0.88083 | 0.43453 |
| C | 2.805728e+00 | 6.151601e+00 | 1.620857e+01 | 0.63817 | 0.62771 | 0.45939 |
| N | 2.794262e+00 | 8.635997e+00 | 1.634353e+01 | 0.76360 | 0.88122 | 0.46322 |
| H | 2.810149e+00 | 3.986347e+00 | 1.641851e+01 | 0.52821 | 0.40677 | 0.46534 |
| H | 3.428580e+00 | 9.304836e+00 | 1.680382e+01 | 0.87105 | 0.94947 | 0.47626 |
| C | 2.817676e+00 | 7.364541e+00 | 1.694646e+01 | 0.70144 | 0.75148 | 0.48030 |
| C | 2.819001e+00 | 4.942136e+00 | 1.695352e+01 | 0.57800 | 0.50430 | 0.48050 |
| C | 2.862114e+00 | 4.935182e+00 | 1.833269e+01 | 0.58263 | 0.50359 | 0.51959 |
| C | 2.790094e+00 | 7.355306e+00 | 1.836703e+01 | 0.69778 | 0.75054 | 0.52057 |
| H | 2.139944e+00 | 9.276044e+00 | 1.849260e+01 | 0.72062 | 0.94654 | 0.52413 |
| H | 2.906531e+00 | 3.975110e+00 | 1.885827e+01 | 0.53878 | 0.40562 | 0.53449 |
| N | 2.752728e+00 | 8.614927e+00 | 1.899090e+01 | 0.75773 | 0.87907 | 0.53825 |
| C | 2.845371e+00 | 6.135346e+00 | 1.909065e+01 | 0.64192 | 0.62606 | 0.54108 |
| H | 2.514826e+00 | 8.583730e+00 | 1.998659e+01 | 0.72863 | 0.87589 | 0.56647 |
| C | 2.868639e+00 | 6.119271e+00 | 2.054050e+01 | 0.64379 | 0.62442 | 0.58217 |
| H | 2.780086e+00 | 4.014053e+00 | 2.089854e+01 | 0.52615 | 0.40960 | 0.59232 |
| H | 2.934782e+00 | 7.087742e+00 | 2.106096e+01 | 0.70085 | 0.72324 | 0.59692 |
| C | 2.836907e+00 | 5.016683e+00 | 2.134984e+01 | 0.58387 | 0.51191 | 0.60511 |
| C | 2.869548e+00 | 5.064496e+00 | 2.278295e+01 | 0.59008 | 0.51679 | 0.64572 |
| H | 2.785949e+00 | 2.953154e+00 | 2.310778e+01 | 0.47270 | 0.30134 | 0.65493 |
| H | 2.921315e+00 | 6.060103e+00 | 2.325464e+01 | 0.64686 | 0.61838 | 0.65909 |
| C | 2.836547e+00 | 3.951963e+00 | 2.356868e+01 | 0.52951 | 0.40326 | 0.66799 |
| S | 2.844662e+00 | 3.825041e+00 | 2.533178e+01 | 0.52397 | 0.39031 | 0.71796 |
| H | 2.921574e+00 | 2.460264e+00 | 2.538159e+01 | 0.46323 | 0.25105 | 0.71938 |
| Au | -3.909631e-02 | 4.951642e-01 | 2.704178e+01 | 0.02074 | 0.05053 | 0.76643 |
| Au | 2.844662e+00 | 4.951642e-01 | 2.704178e+01 | 0.35408 | 0.05053 | 0.76643 |
| Au | 5.728420e+00 | 4.951642e-01 | 2.704178e+01 | 0.68741 | 0.05053 | 0.76643 |
| Au | -1.480975e+00 | 2.992572e+00 | 2.704178e+01 | -0.01850 | 0.30536 | 0.76643 |
| Au | 1.402783e+00 | 2.992572e+00 | 2.704178e+01 | 0.31483 | 0.30536 | 0.76643 |
| Au | 4.286541e+00 | 2.992572e+00 | 2.704178e+01 | 0.64816 | 0.30536 | 0.76643 |
| Au | -2.922855e+00 | 5.489980e+00 | 2.704178e+01 | -0.05775 | 0.56020 | 0.76643 |
| Au | -3.909631e-02 | 5.489980e+00 | 2.704178e+01 | 0.27558 | 0.56020 | 0.76643 |
| Au | 2.844662e+00 | 5.489980e+00 | 2.704178e+01 | 0.60892 | 0.56020 | 0.76643 |
| Au | -3.909631e-02 | 2.160103e+00 | 2.939636e+01 | 0.10569 | 0.22042 | 0.83316 |
| Au | 2.844662e+00 | 2.160103e+00 | 2.939636e+01 | 0.43902 | 0.22042 | 0.83316 |
| Au | 5.728420e+00 | 2.160103e+00 | 2.939636e+01 | 0.77236 | 0.22042 | 0.83316 |
| Au | -1.480975e+00 | 4.657511e+00 | 2.939636e+01 | 0.06644 | 0.47526 | 0.83316 |
| Au | 1.402783e+00 | 4.657511e+00 | 2.939636e+01 | 0.39978 | 0.47526 | 0.83316 |

```
Au    4.286541e+00  4.657511e+00  2.939636e+01    0.73311  0.47526  0.83316
Au   -2.922855e+00  7.154919e+00  2.939636e+01    0.02719  0.73009  0.83316
Au   -3.909631e-02  7.154919e+00  2.939636e+01    0.36053  0.73009  0.83316
Au    2.844662e+00  7.154919e+00  2.939636e+01    0.69386  0.73009  0.83316
Au    1.402783e+00  1.327634e+00  3.175093e+01    0.22988  0.13547  0.89990
Au    4.286541e+00  1.327634e+00  3.175093e+01    0.56322  0.13547  0.89990
Au    7.170299e+00  1.327634e+00  3.175093e+01    0.89655  0.13547  0.89990
Au   -3.909631e-02  3.825041e+00  3.175093e+01    0.19064  0.39031  0.89990
Au    2.844662e+00  3.825041e+00  3.175093e+01    0.52397  0.39031  0.89990
Au    5.728420e+00  3.825041e+00  3.175093e+01    0.85730  0.39031  0.89990
Au   -1.480975e+00  6.322449e+00  3.175093e+01    0.15139  0.64515  0.89990
Au    1.402783e+00  6.322449e+00  3.175093e+01    0.48472  0.64515  0.89990
Au    4.286541e+00  6.322449e+00  3.175093e+01    0.81806  0.64515  0.89990
Au   -3.909631e-02  4.951642e-01  3.410551e+01    0.02074  0.05053  0.96663
Au    2.844662e+00  4.951642e-01  3.410551e+01    0.35408  0.05053  0.96663
Au    5.728420e+00  4.951642e-01  3.410551e+01    0.68741  0.05053  0.96663
Au   -1.480975e+00  2.992572e+00  3.410551e+01   -0.01850  0.30536  0.96663
Au    1.402783e+00  2.992572e+00  3.410551e+01    0.31483  0.30536  0.96663
Au    4.286541e+00  2.992572e+00  3.410551e+01    0.64816  0.30536  0.96663
Au   -2.922855e+00  5.489980e+00  3.410551e+01   -0.05775  0.56020  0.96663
Au   -3.909631e-02  5.489980e+00  3.410551e+01    0.27558  0.56020  0.96663
Au    2.844662e+00  5.489980e+00  3.410551e+01    0.60892  0.56020  0.96663
```

# References


[S1] S. Datta, *Electronic Transport in Mesoscopic Systems*. Cambridge Studies in Semiconductor Physics, Cambridge University Press, Cambridge, 1997.

[S2] A. A. Gorbatsevich and N. M. Shubin, "Unified theory of resonances and bound states in the continuum in hermitian tight-binding models," *Phys. Rev. B*, vol. 96, p. 205441, Nov 2017.

[S3] J. Sherman and W. J. Morrison, "Adjustment of an inverse matrix corresponding to a change in one element of a given matrix," *The Annals of Mathematical Statistics*, vol. 21, no. 1, pp. 124–127, 1950.

[S4] D. A. Harville, *Matrix algebra from a statistician's perspective*, vol. 1. Springer, New York, NY, 1997.

[S5] F. Goyer, M. Ernzerhof, and M. Zhuang, "Source and sink potentials for the description of open systems with a stationary current passing through," *The Journal of Chemical Physics*, vol. 126, no. 14, p. 144104, 2007.

[S6] B. Pickup and P. Fowler, "An analytical model for steady-state currents in conjugated systems," *Chemical Physics Letters*, vol. 459, no. 1, pp. 198 – 202, 2008.

[S7] T. Stuyver, S. Fias, F. De Proft, P. Geerlings, Y. Tsuji, and R. Hoffmann, "Enhancing the conductivity of molecular electronic devices," *The Journal of Chemical Physics*, vol. 146, no. 9, p. 092310, 2017.

[S8] B. Hourahine, B. Aradi, V. Blum, F. Bonafe, A. Buccheri, C. Camacho, C. Cevallos, M. Y. Deshaye, T. Dumitrica, A. Dominguez, S. Ehlert, M. Elstner, T. van der Heide, J. Hermann, S. Irle, J. J. Kranz, C. Kohler, T. Kowalczyk, T. Kubar, I. S. Lee, V. Lutsker, R. J. Maurer, S. K. Min, I. Mitchell, C. Negre, T. A. Niehaus, A. M. N. Niklasson, A. J. Page, A. Pecchia, G. Penazzi, M. P. Persson, J. Rezac, C. G. Sanchez, M. Sternberg, M. Stohr, F. Stuckenberg, A. Tkatchenko, V. W.-z. Yu, and T. Frauenheim, "Dftb+, a software package for efficient approximate density functional theory based atomistic simulations," *The Journal of Chemical Physics*, vol. 152, no. 12, p. 124101, 2020.

[S9] A. Fihey, C. Hettich, J. Touzeau, F. Maurel, A. Perrier, C. Kohler, B. Aradi, and T. Frauenheim, "Scc-dftb parameters for simulating hybrid gold-thiolates compounds," *Journal of Computational Chemistry*, vol. 36, no. 27, pp. 2075–2087, 2015.

[S10] D. Ryndyk, R. Gutiérrez, B. Song, and G. Cuniberti, "Green function techniques in the treatment of quantum transport at the molecular scale," in *Energy Transfer Dynamics in Biomaterial Systems*, pp. 213–335, Springer, Berlin, Heidelberg, 2009.

[S11] S. Smidstrup, T. Markussen, P. Vancraeyveld, J. Wellendorff, J. Schneider, T. Gunst, B. Verstichel, D. Stradi, P. A. Khomyakov, U. G. Vej-Hansen, M.-E. Lee, S. T. Chill, F. Rasmussen, G. Penazzi, F. Corsetti, A. Ojanperä, K. Jensen, M. L. N. Palsgaard, U. Martinez, A. Blom, M. Brandbyge, and K. Stokbro, "QuantumATK: an integrated platform of electronic and atomic-scale modelling tools," *Journal of Physics: Condensed Matter*, vol. 32, p. 015901, oct 2019.

[S12] J. P. Perdew and Y. Wang, "Accurate and simple analytic representation of the electron-gas correlation energy," *Phys. Rev. B*, vol. 45, pp. 13244–13249, Jun 1992.

[S13] J. P. Perdew, K. Burke, and M. Ernzerhof, "Generalized gradient approximation made simple," *Phys. Rev. Lett.*, vol. 77, pp. 3865–3868, Oct 1996.

[S14] M. van Setten, M. Giantomassi, E. Bousquet, M. Verstraete, D. Hamann, X. Gonze, and G.-M. Rignanese, "The pseudodojo: Training and grading a 85 element optimized norm-conserving pseudopotential table," *Computer Physics Communications*, vol. 226, pp. 39 – 54, 2018.

[S15] K. Momma and F. Izumi, "*VESTA3* for three-dimensional visualization of crystal, volumetric and morphology data," *Journal of Applied Crystallography*, vol. 44, pp. 1272–1276, Dec 2011.

[S16] A. F. Sadreev, E. N. Bulgakov, and I. Rotter, "Bound states in the continuum in open quantum billiards with a variable shape," *Phys. Rev. B*, vol. 73, p. 235342, Jun 2006.

[S17] L. Jin and Z. Song, "A physical interpretation for the non-hermitian hamiltonian," *Journal of Physics A: Mathematical and Theoretical*, vol. 44, no. 37, p. 375304, 2011.

[S18] K. G. L. Pedersen, A. Borges, P. Hedegård, G. C. Solomon, and M. Strange, "Illusory connection between cross-conjugation and quantum interference," *The Journal of Physical Chemistry C*, vol. 119, no. 48, pp. 26919–26924, 2015.

[S19] L. A. Zotti and E. Leary, "Taming quantum interference in single molecule junctions: induction and resonance are key," *Phys. Chem. Chem. Phys.*, vol. 22, pp. 5638–5646, 2020.

[S20] T. Markussen, R. Stadler, and K. S. Thygesen, "The relation between structure and quantum interference in single molecule junctions," *Nano Letters*, vol. 10, no. 10, pp. 4260–4265, 2010. PMID: 20879779.

[S21] Y. Tsuji and K. Yoshizawa, "Frontier orbital perspective for quantum interference in alternant and nonalternant hydrocarbons," *The Journal of Physical Chemistry C*, vol. 121, no. 17, pp. 9621–9626, 2017.

[S22] H. Friedrich and D. Wintgen, "Interfering resonances and bound states in the continuum," *Phys. Rev. A*, vol. 32, pp. 3231–3242, Dec 1985.

[S23] M. L. L. d. Guevara, F. Claro, and P. A. Orellana, "Ghost fano resonance in a double quantum dot molecule attached to leads," *Phys. Rev. B*, vol. 67, p. 195335, May 2003.